ผลของสารก่อผลึกบีตาและตัวเติมแร่ที่มีต่อสมบัติเชิงกลของพอลิเมอร์ผสมพีพี/อีพีอาร์

นางสาว รัชนีกุล บุญหนูกลับ

EFFECTS OF β-NUCLEATING AGENT AND MINERAL FILLERS ON
MECHANICAL PROPERTIES OF PP/EPR BLENDS

Miss Ratchaneekun Bunnuklap

Thesis Title	Effects of β-Nucleating Agent and Mineral
	Fillers on Mechanical Properties of PP/EPR Blends
By	Miss Ratchaneekun Bunnuklap
Field of Study	Petrochemistry and Polymer Science
Thesis Advisor	Associate Professor Supawan Tantayanon, Ph.D
Thesis Co-Advisor	Assistant Professor Pitt Supaphol, Ph.D.

Accepted by the Faculty of Science, Chulalongkorn University in Partial Fulfillment of the Requirements for the Master's Degree
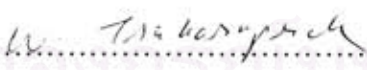
....Dean of the Faculty of Science

(Professor Piamsak Menasveta, Ph.D.)

THESIS COMMITTEE

....Chairman

(Professor Pattarapan Prasassarakich, Ph.D.)

....Thesis Advisor

(Associate Professor Supawan Tantayanon, Ph.D.)

....Thesis Co-advisor

(Assistant Professor Pitt Supaphol, Ph.D.)

....Member

(Associate Professor Wimonrat Trakarnpruk, Ph.D.)

....Member

(Assistant Professor Varawut Tangpasuthadol, Ph.D.)

รัชนีกุล บุญหนูกลับ: ผลของสารก่อผลึกบีตาและตัวเติมแร่ที่มีต่อสมบัติเชิงกลของพอลิเมอร์ผสมพีพี/อีพีอาร์ (EFFECTS OF β-NUCLEATING AGENT AND MINERAL FILLERS ON MECHANICAL PROPERTIES OF PP/EPR BLENDS)อ.ที่ปรึกษา: รศ. ดร.ศุภวรรณ ตันตยานนท์, อ.ที่ปรึกษาร่วม: ผศ. ดร.พิชญ์ ศุภผล, 74 หน้า ISBN 974-17-3830-7

งานวิจัยนี้จัดทำขึ้นเพื่อศึกษาผลของสารก่อผลึกแบบบีตาและสารตัวเติมในพีพี/อีพีอาร์เบลนด์ โดยสารก่อผลึกที่ใช้คือของผสมของแคลเซียมสเตียเรตและไพมีลิกแอซิด กับ ของผสมของแคลเซียมสเตียเรตและซับมีลิกแอซิด ปริมาณ 0.001 เปอร์เซ็นต์โดยน้ำหนัก และสารตัวเติมที่ใช้คือ เคโอลินและแคลเซียมคาร์บอเนต เมื่อวิเคราะห์ด้วยเครื่อง WAXD พบว่า เฉพาะสารก่อผลึกของผสมของแคลเซียมสเตียเรตและไพมีลิกแอซิดเท่านั้นที่ให้ผลึกแบบบีตา สำหรับผลของสารตัวเติมพบว่า การเติมแคลเซียมคาร์บอเนตในปริมาณ 5, 10, 15 เปอร์เซ็นต์โดยน้ำหนักในพีพี/อีพีอาร์เบลนด์ ทำให้เกิดผลึกแบบบีตา รวมทั้งปรับปรุงค่าโมดูลัสและโมดูลัสยืดหยุ่นให้สูงขึ้น ดังนั้น ได้เติมของผสมของแคลเซียมสเตียเรตและไพมีลิกแอซิดกับแคลเซียมคาร์บอเนตในพีพี/อีพีอาร์เบลนด์ พบว่าที่ 0.001 เปอร์เซ็นต์โดยน้ำหนักของผสมของแคลเซียมสเตียเรตและไพมีลิกแอซิด และ 5 เปอร์เซ็นต์โดยน้ำหนักของแคลเซียมคาร์บอเนตขนาดนาโนเมตร ให้ค่าความทนแรงกระแทกสูงสุด และให้ค่าโมดูลัสและโมดูลัสยืดหยุ่นเพิ่มขึ้น และให้ค่า k-value ประมาณ 0.3 ซึ่งมีค่ามากกว่าแคลเซียมคาร์บอเนตที่ไม่ได้เติมของผสมของแคลเซียมสเตียเรตและไพมีลิกแอซิด แสดงว่าทั้งของผสมของแคลเซียมสเตียเรตและไพมีลิกแอซิด และแคลเซียมคาร์บอเนตทำให้เกิดผลึกบีตา และจากการศึกษาสมบัติทางความร้อนของของผสมนี้ ด้วยเครื่อง DSC พบว่ามีจุดหลอมเหลวของผลึกบีตาที่ 153 องศาเซลเซียส เมื่อทำการศึกษาการเกิดผลึกบีตาที่อุณหภูมิตกผลึกคงที่ 130 องศาเซลเซียส พบว่าการเติมของผสมของแคลเซียมสเตียเรตและไพมีลิกแอซิด 0.001 เปอร์เซ็นต์โดยน้ำหนักและแคลเซียมคาร์บอเนตขนาดนาโนเมตรที่ 10 เปอร์เซ็นต์โดยน้ำหนักในพีพี/อีพีอาร์เบลนด์ ให้ค่า k-value เท่ากับ 1 ซึ่งแสดงถึงการเกิดบีตาที่สมบูรณ์

สาขาวิชา ปิโตรเคมีและวิทยาศาสตร์พอลิเมอร์ ลายมือชื่อนิสิต ....

ปีการศึกษา 2548 ลายมือชื่ออาจารย์ที่ปรึกษา ....

ลายมือชื่ออาจารย์ที่ปรึกษาร่วม ....

4573410223: MAJOR PETROCHEMISTRY AND POLYMER SCIENCE

KEYWORD: ISOTACTIC POLYPROPYLENE/β-NUCLETOR/β-PP/EPR BLEND / CALCIUM CARBONATE NANOCOMPOSITE

RATCHANEEKUN BUNNUKLAP: EFFECTS OF β-NUCLEATING AGENT AND MINERAL FILLERS ON MECHANICAL PROPERTIES OF PP/EPR BLENDS. THESIS ADVISOR: ASSOC. PROF. SUPAWAN TANTAYANON, Ph.D., THESIS CO-ADVISOR: ASST. PROF. PITT SUPAPHOL, Ph.D., 74 pp. ISBN: 974-17-3830-7

The effect of nucleating agents (0.001 wt% bicomponent of calcium stearate and pimelic acid, Ca-Pim, and 0.001 wt % bicomponent of calcium stearate and suberic acid, Ca-Sub) and fillers (kaolin and $CaCO_3$) on β-crystalline in PP/EPR blend were investigated by WAXD measurement. Results showed that only Ca-Pim promoted β-crystalline. For the fillers, it was found that 5-15 wt% of calcium carbonate promoted β-crystalline and improved tensile and flexural moduli. Therefore, both Ca-Pim and $CaCO_3$ were simultaneously added into the PP/EPR blend in order to improve its Izod impact, tensile modulus and flexural modulus. It was found that the composite containing 0.001 wt% Ca-Pim and 5 wt% nano-$CaCO_3$ had the highest impact strength and high tensile and flexural moduli. From WAXD measurement, the k-value was about 0.3, higher than that of $CaCO_3$ without Ca-Pim. It indicated that both Ca-Pim and $CaCO_3$ additively promoted β-crystallization. The β-crystalline formation was also confirmed by DSC which exhibited an endothermic melting peak at $153^{\circ}C$. The effect of isothermal crystallization of Ca-Pim and $CaCO_3$ at 130 $^{\circ}C$ on β-crystalline, thermal properties and spherulitic structure was investigated. The results showed k-value of 0.001 wt% Ca-Pim and 10 wt % nano-$CaCO_3$ wt. was 1.0, indicating that β-crystalline occurred completely.

Field of study Petrochemistry and Polymer Science Student's signature Ratdanakun B.

Academic year 2005 Advisor's signature

Co-advisor's signature

ACKNOWLEDGEMENTS

CONTENTS

LIST OF FIGURES

Figure																																			Page

LIST OF TABLES

Table   Page

LIST OF ABBREVIATIONS

iPP   : isotactic polypropylene

PP   : polypropylene

α-form   : alpha-form

β-form   : beta-form

γ-form   : gamma-form

EPR/PP blends   : ethylene-propylene rubber blends

Ca-Pim   : calcium stearate and pimelic acid

Ca-Sub   : calcium stearate and suberic acid

$CaCO_3$: calcium carbonate

μm-$CaCO_3$: micrometer- calcium carbonate

nm- $CaCO_3$: nanometer- calcium carbonate

T_m : melting temperature

T_c : crystallization temperature

wt.%   : percentage by weight

WAXD   : wide angle x-ray diffraction

DSC   : differential scanning calorimetry

CHAPTER I

INTRODUCTION

1.1 Statement of problem

Isotactic polypropylene (PP) is becoming the most important commodity polymer widely used in technical applications .Because of its good mechanical properties, its facile processing, its versatility to accept numerous types of filler, and its relatively low cost. PP has found a wide range of applications in the houseware, package, and automotive industries. Despite its simple molecular structure, its mechanical properties depend on the supermolecular structure arrangement achieved in crystalline state. Isotactic polypropylene is known to exhibit four different crystalline forms; α-form, β-form, γ-form and smectic. Under normal processing conditions, α-PP is the principal constituent which may be accompanied by the relatively low amount of β modification. The formation of β-PP can be promoted in PP by adding various β nucleators such as quinacridone dye, calcium carbonate or wallastonite. The most beneficial selectivity and activity were found for calcium salts of pimelic (Ca-Pim) and suberic (Ca-Sub) acids. The β-form PP exhibits a higher impact energy but lower yield strength and elastic modulus than α- PP.

The incorporation of calcium carbonate, mica or talc as a filler in thermoplastics is a common practice in plastic industries for the reduction of production costs of molded products. It is well known that minerals fillers improve the rigidity of the polymers, but they also decrease ductility and toughness. In this work we have studied on the effect of calcium carbonate addition on the mechanical properties of β-PP.

1.2 Objective

The main purpose of this study is therefore to focused on studying the effect of the nucleating agent (Ca-Pim and Ca-Sub) and fillers on crystalline structure, thermal properties and mechanical properties of PP/EPR blends

1.3 Scope of the research

The scope of this research work includes

1. Survey of literature and supplying of source of the selected β-nucleator and filler such as quinacridone, calcium carbonate, talc, etc.

2. Preliminary investigating the effect of β-nucleator on mechanical properties of PP/EPR blends.

3. Preparation of resin compounds by blending PP with the selected β-nucleator and filler using twin-screw extruder.

4. Evaluation of the β-crystalline using wide angle X-ray diffraction (WAXD) technique.

5. Study of the β-crystalline and filler on mechanical properties, especially impact strength.

6. Evaluation of the thermal properties of β-crystalline sample using differential scanning calorimetry (DSC).

7. Observation of the spherulitic structure of β-crystalline sample using polarizing microscope.

8. Summarizing the results including discussion.

CHAPTER II

THEORY AND LITERATURE REVIEW

2.1 Polypropylene growth and use

Polypropylene was initially produced commercially about 45 years ago after the successful development of a suitable stereo-specific catalyst, which enabled the polymer to have a kind of structural characteristics useful for rigid items. The continuous growth of polypropylene is expected to continue into the next millennium as raw materials in an expanding number of end-use products for the automotive and film industries.[1] Earlier, the performance of polypropylene was considered intermediate to polyethylene and polystyrene (PS). But, as a late, there is significant intermaterial competition to replace engineering polymers as materials of construction by polypropylene base resin.

The significant growth of PP use is attributed to combination of many factors besides a good balance in physical and chemical properties. Because of the appropriate melt rheology and thermal behavior, PP-based materials are widely processable on a variety of different equipment ranging from injection molding to some designed for the use in order industries, like calendaring and air-quenched blow film equipment. Additionally, by the having the lowest density among commodity plastics at approximately 0.90 g/cm^3, continued market penetration of PP at the current rate of growth is almost ensured on the basis of good mechanical properties at reduced cost per volume. Finally, because many major companies are designing their products, polypropylene stands out as the main product with the widest design flexibility and simplicity of recycling. Its excellent thermal stability, low density (assisting in separating from other materials), chemical and environmentalinertness, even its caloric in the case of incineration all add to its attractiveness as the material of construction

The global supply from several producers located throughout the world ensures good supply at competitive prices. From the mid-1990s to the end of the 20th century, significant capacity increases will occur. The supply and demand balance works favorably to the consumer's benefit. This keeps prices in check and ensure that the suitable supply will be available. Additionally, in the next 10 years, significant amounts of polypropylene from recycled material varies widely in cleanliness but is thought to be suitable for a variety of applications, including operation, and this will continue. Additionally, postconsumer waste primarily from packaging is becoming more available but often of lower quality (e.g., sometimes limited to black pigmented products).

Polypropylene homopolymer consists of molecular chains with repeating unit of propylene monomer generated in the reactor. It is derived from three major sources today. Globally, most propylene monomer comes from the stream cracking processusing naphtha, a valuable fraction of crude oil. Usually, naphtha crackers target products are ethylene monomer. Propylene is a by product of the cracking process produced at various ratios depending on the crude oil feedstock. Many cracking processes have a propylene plant intimately connected effectively use the propylene that comes from naphtha cracking. The second largest production of propylene comes from the gasoline refining process.

Finally, and most recently, a new process by which propane is dehydrogenated to propylene monomer has been used to produce propylene. Despite certain economical short coming, when propane is readily available and transportation to markets is less favorable, this process is now starting to be applied. Propylene purity requirement for the production of polymers is very high. Trace impurities in the polymerization process cause poisoning of the catalyst during production. The industrial routes to produce propylene monomer and the region capacities with expected growth are outlined in Figure 2.1.[1]
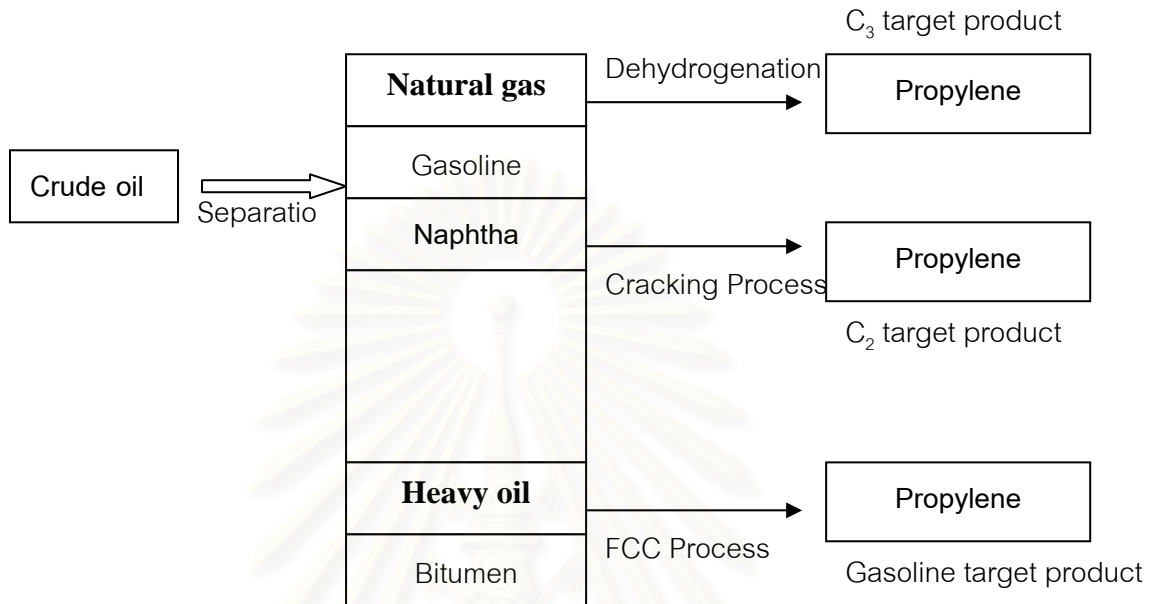
Figure 2.1 Supply of polypropylene monomer.[1]

2.2 Isotactic polypropylene (iPP)

2.2.1 Structure and morphology

Polypropylene is one of the most important of hydrocarbon polymers and is the first synthetic stereoregular polymer to achieve considerable commercial and industrial importance.

Stereoregular polypropylene was first obtained by Natta and co-workers in the 1950s that the chain conformation of iPP is a threefold helix, which can be either right or left-handed, with a periodicity of 6.5 $^{\circ}$A.

$$\left(-CH_2-CH-\right)_n$$
$$\qquad\qquad | $$
$$\qquad\qquad CH_3$$
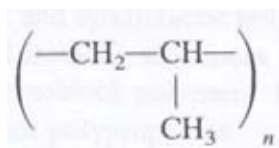
The molecular structure of polypropylene is formally derived from polyethylene by the substitution of one of the H atoms on alternate C atom of the chain by CH_3 group. Stereoregular configuration can be described as Figure 2.2. Figure 2.2*a* is isotactic, in which all pendant CH_3 groups are attached on the same side of the chain, that is, all units have a spatially identical arrangement of atom; Figure 2.2*b* is syndiotactic, in which the configuration of the C atom carrying the side group shows a regular alternation along the chain; Figure 2.2*c* is atactic, which there is a random arrangement of pendant CH_3 groups [2].
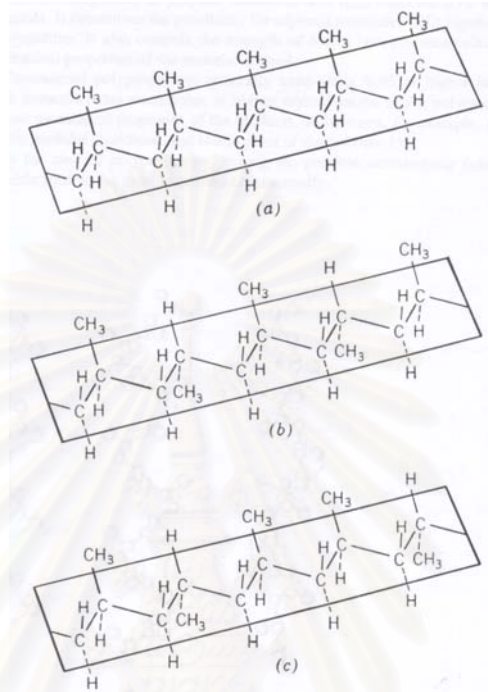
Figure 2.2 Representation of the spatial disposition of CH₃ in (a) isotactic, (b) syndiotactic, and (c) atactic polypropylene chain segment [2].
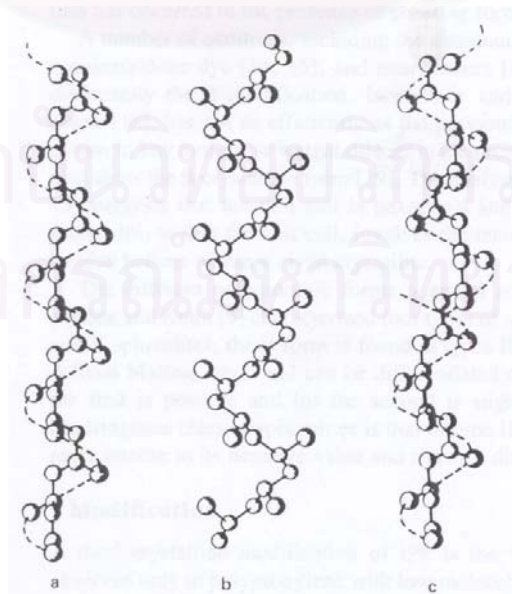
Figure 2.3 Models of (a) isotactic (b) syndiotactic (c) stereobloc iPP [2].

The stereoregularity of polymer molecules is of high importance for the properties of materials. It determines the possibility for adjacent molecules to fit together and therefore to crystallize. It also controls the strength of forces between molecules, on which the mechanical properties of the material depends.

Commercial polypropylenes generally have about 0.95 or higher isotactic indices. High isotactic index contributes to higher crystallization of the polymer and much improved mechanical properties of the products. It increase, for example, the yield stress, elastic modulus, hardness, and brittle point of the polymer.

The crystallizability of the chain is a critical factor governing the resultant morphology. The degree of crystallinity of PP homopolymer is governed primarily by the tacticity of the chain. Isotactic chains result from the head-to-tail addition of polypropylene monomer units, where the methyl groups always have the same configuration with respect to the polymer backbone, Syndiotactic chains result from the same head-to-tail addition of monomer units, but the methyl groups have the alternating configuration with respect to polymer backbone. The stereospecificity (isospecifc or syndiospecific) refers to the consistent placement of the methyl group placement. Atactic chains do not have any consistent placement of the methyl groups. Figure 2.3 shows a schematic of isotactic, syndiotactic and atactic PP chains.

The stereochemistry of the PP chain strongly influences the crytallinity. This is show in Figure 2.4, which shows wide angle X-ray patterns of isotactic, syndiotactic and atactic PP. Figure 2.4 shows pronounced crystalline reflections when the PP chain contains either regular isotactic or syndiotactic sequences. Those patterns are related to the specific crystal unit cell symmetries for the isotactic and syndiotactic PP. Atactic PP shows no strong reflections, exhibiting only a very broad and diffuse scattering from X-rays that is characteristic of a noncrystalline material.

On the crystal lattice level, isotactic PP shows well-known crystalline forms, namely monoclinic: α-form, hexagonal: β-form, triclinic: γ-form and smectic: δ-form (partial order of micro crystal of the hexagonal and/or monoclinic). The α-form dominates in the crystallization of the PP grades used in mostly industrial

applications. Among these four crystalline structures the β-form demonstrates higher performance such as higher tensile elongation and higher impact resistance.
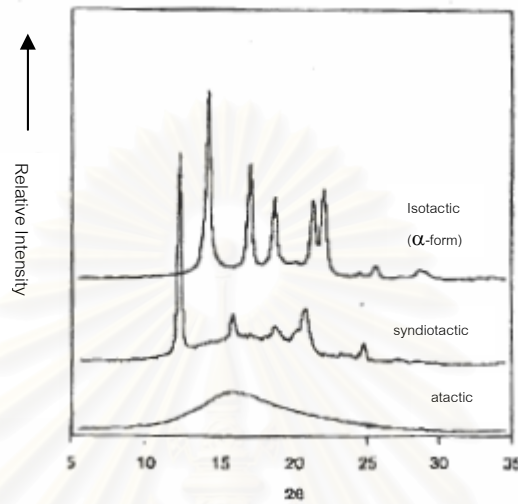
Figure 2.4 Wide angle X-ray patterns of isotactic, syndiotactic and atactic PP [2].

2.2.2 α Modification

The principal isotactic form (the α form) was first observed by Natta in melt crystallized material. It is normally observed also in solution-grown crystals. The structure determinations carried out on α phase isotactic polypropylene showed that the crystal structure is monoclinic and the chains assume a helical conformation. From the x-ray data it follows that that the identity in the main direction of the chain comprise three monomer units. The symmetry of the helix is characterized by a threefold screw axis. Consequently right-and left-handed helices are possible. They are arranged in a regular pattern, a left-handed helix always facing a right-handed one [2].

2.2.3 β Modification

Commercial grades of iPP, when processed in laboratory or industrial scale, crystallize essentially into α-modification. At first Padden and colleagues [3] demonstrated by X-ray diffractometric and optical microscopic studies that, at the high supercooling, the formation of the α- modification was accompanied by appearance of the β- modification. Soon after, this observation was reported by other researchers [4, 5].

Turner Jones, Aizlewood and Beckett [6] were the first to report the formation of samples highly rich in β- modification. They crystallized a particular (unspecified) IPP sample in the range of 393-403 K into nearly pure β-IPP. They introduced a k value for characterizing the proportion of β- modification by X-ray diffractometric data, as follows; [7]

$$k = \frac{H_{\beta 1}}{H_{\beta 1} + (H_{\alpha 1} + H_{\alpha 2} + H_{\alpha 3})}$$

where $H_{\alpha 1}$, $H_{\alpha 2}$, $H_{\alpha 3}$ are intensities of α-diffraction peaks corresponding to angle $\theta = 7.1^{\circ}$, 8.5°, and 9.4°, respectively , and $H_{\beta 1}$ is the intensity of β-diffraction peaks corresponding to angle $\theta = 8.1^{\circ}$. The K-value is relative measure for characterizing the polymorphic composition but it does not express the absolute value of β-content numerically, although its value is 0 for α-IPP and 1 for β-IPP, as is apparent .

Several attempts were subsequently made to prepare the β-modification in pure form. Two methods have been used successfully to prepare samples rich in β-modification; the temperature gradient method [8-10] and introduction of β-nucleating agents [11-14]. Furthermore, it is known that shear stress also promotes the formation of β-modification [15-16].

The use of nucleating agent can affect the physical and/or optical properties of PP products. Regardless of which effect is desired, it is brought about by the same mechanism; increased nucleation of the crystallizing PP. In general, PP can crystalline form, depending on the nucleating agent type which is used. Typical nucleating agents are shown in following Table 2.4.

Table 2.1 Nucleator types [34]

Nucleator types	Crystal form provided
1) Lithium, sodium, potassium benzoate	α-crystalline form
2) Sodium salts or organophosphates	
3) Talcum, finely divided(<40 nm) clays	
4) Millad, bis-(3,4-dimethylbenzylidene sorbitol diacetal)	
5) Quinacridone dye	β-crystalline form
6) Triphenol ditrazine	
7) Aluminium quinizarin sulfonic acid	
8) Disodium, calcium phthalate	
9) Wallastonite	

The β-form PP is easily identified by X-ray diffraction, polarized optical microscopy, and scanning electron microscopy due to its high birefringence. The β-form has been obtained by crystallization at higher temperatures (T_c= 120-140°C)

and can only be studied if the sample temperature is maintained above 110°C. Moreover, β-crystallization I reduced in copolymers of propylene with ethylene [5].

Numerous investigations have been carried out involving the subject of the β-iPP crystal structure but most previous studies were only concentrated on the technique that obtains a higher level of the β-form and on the morphology. Three techniques are used to promote the β-form are the follwing:

1. Addition of β-nucleators.

2. Crystallization in a temperature gradient/thermal gradient.

3. Shear-induced technique.

Crystallization in the presence of β-nucleating agents promises to be the most reliable method for industrial applications. The most well known and widespread β-nucleating agents is a γ-quinacridone red pigment (Permanent Rot E3B) as an effective nucleating agent. Their k value is around 0.8 as calculated from X-ray diffractometric data but, when crystallized under given thermal conditions, k may reach about 0.9 [7]. Even though γ-quinacridone is one of the most effective β-nucleating agent, pure β-IPP could not be prepared in its presence. In other words, its α-nucleating effect is not negligible. It was also observed that its β-nucleating activity is reduced during processing. This indicates a modification in the physical or chemical structure of this red pigment due to the high pressure and temperature of processing. A drawback of γ-quinacridone is its intense red colour, which may restrict its practical application.

The internal microstructure of the β-form spherulites is thought to be composed of radial arrays of parallel stacked lamellae. In this regard, the lamellar microstructure of the β-form exhibits much greater similarity to the conventional microstructure of semicrystalline homopolymers than does the α-form with its unique tendency for cross-hatch formation. Various studies have suggested that the crystallographic *a*-axis direction, assuming a hexagonal unit cell [17].

Various mechanisms have been postulated for β-form melting and the β- to α-form recrystallization process. Many of the associated effects bear close resemblance to general reorganization phenomena in semicrystalline polymers. Varga and co-workers have extensively investigated and reviewed the transition of β-form to α-form crystallinity in optical microscopy and DSC experiments. Using preferentially nucleated materials, these studies suggested that the optimum isothermal crystallization temperature for formation of β-crystallinity is between 100 $^{\circ}$C and 141 $^{\circ}$C [18]. It was proposed that recrystallization of the β-form to α-form is promoted if the temperature is lowered, following crystallization, below critical temperature. This critical temperature, *TR**, was in the range of 100 $^{\circ}$C to 110 $^{\circ}$C [19]. The proposed mechanism was thought to occur by formation of α-form nuclei within the β-spherulite after cooling below *TR**. The α-form nuclei act as sites for α-form recrystallization following melting of metastable β-form crystallites on heating. Figure 2.5 and 2.6 show typical X-ray diffraction diagrams. Figure 2.9 shows optical micrograph of pure β-IPP crystallized [7].
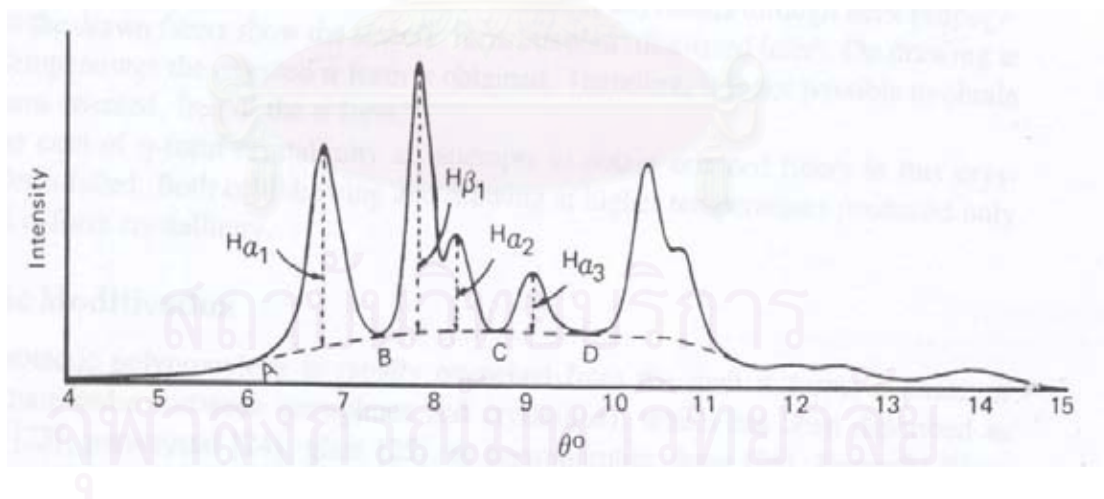
Figure 2.5 X- ray diffraction diagrams showing mixed α and β crystalline [14].
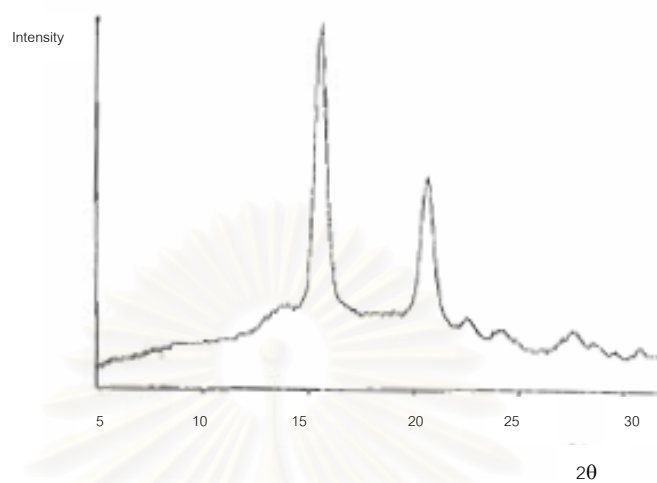
Figure 2.6 X- ray diffractogram of pure β-IPP [14].

Figure 2.7 Optical micrograph of pure β-IPP crystallized at Tc= 398 K [14].

2.2.4 γ-Modification

The third crystalline modification of IPP is γ-form. It was first described [3] as observed only in polypropylene with low molecular weight having a degree of isotacticity not too low. It was later obtained from solvent fractionation [2]. A

fraction of isotactic polypropylene precipitated from petrol ether or xylene in the temperature range 35-70 $^{\circ}$C, melted and slowly cooled from 190 $^{\circ}$C, under vacuum, at 6 $^{\circ}$/hr to room temperature, shows γ-form crystallinity. It is therefore not necessarily associated with low molecular weight polymer cystallinity.

This crystalline modification has been obtained, free of α form, by melt crystallization under conditions of elevated pressure. In this case a difference in behavior was found between specimen prepared at a large degree of supercooling ($\Delta t > 40$ $^{\circ}$C) and at a low degree supercooling ($\Delta t < 40$ $^{\circ}$C). In the first case the samples, examined by low-angle X-ray diffraction, show long spacings, which are characteristic of chain-folded lamellar crystals. For the second one, no long spacings are obtained. These data suggest that for the samples prepared at elevated pressure with low supercooling the amount of chain folding is minimal. It is suggested that in this case the γ phase is composed by extended chain crystallization.

The most likely unit cell for the γ form is triclinic. The method of crystallization and the molecular weight of the sample play an important role in determining the phases present in the sample.

Figure 2.8 presents the X-ray diffraction diagrams of three crystalline form of isotactic polypropylene.

The γ phase polypropylene crystallized at elevated hydrostatic is metastable in character. The DSC thermogram of a sample crystallized under pressure at a large degree of supercooling shows that material transforms entirely to the α phase prior to melting. On the contrary, when the γ phase is prepared with low degree of supercooling it is stable, showing no transformation t o the α phase up to 173 $^{\circ}$C, temperature at which the X-ray scan obtained showed only the presence of γ phase [2].
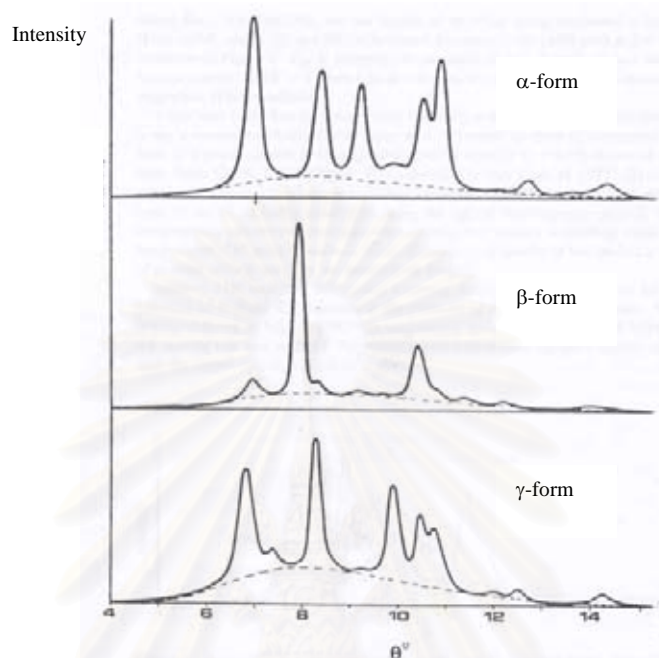
Figure 2.8 X- ray diffraction diagrams of iPP crystalline forms [2].

2.2.5 Smectic

Many commercial fabrication process utilize rapid cooling conditions. Under these conditions, it is common to observe the crystallization of IPP in to the mesomorphic form, also commonly referred to as the smectic form. The mesomorphic phase represents a state of order intermediate between the amorphous and crystalline states. Figure 2.9 shows a comparison of the wide angle X-ray pattern of the mesomorphic form compared to the patterns of atactic PP (amorphous) and the α-form of IPP.

Early work suggested a hexagonal crystallographic symmetry in the mesomorphic form [20]. This assignment of the hexagonal structure was based on the observation that the primary diffraction intensity maxima of the mesomorphic form more closely corresponded to the two most intense reflections of the β-form, which was classified as a hexagonal unit cell. The mesomorphic form could be induced by compressive deformation of IPP in the α-form, provided that the

deformation temperature was below the upper stability limit of the mesomorphic form. Similarly, some experiments have suggested that an oriented mesomorphic form results from drawing samples with β-form crystallinity at low temperature [20].
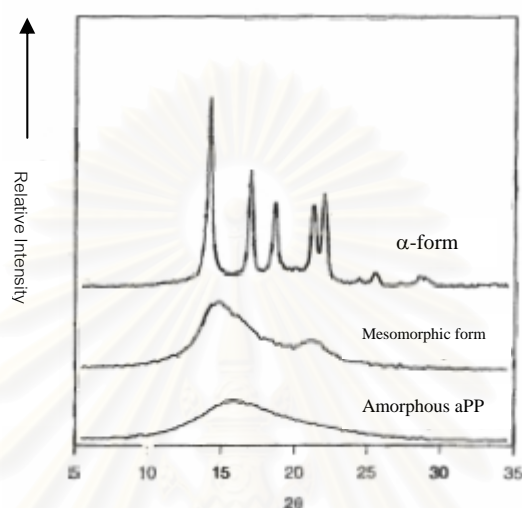
Figure 2.9 A comparison of the WAXD pattern of the aPP (amorphous), iPP in the and the mesomorphic form , and iPP in the α-form [2].

2.2.6 Impact-Modified PP

Polypropylene homopolymer, while having a number of valuable properties and economic benefits, exhibits a poor low-temperature impact resistance. Such a shortcoming is due to its relatively high glass transition temperature (T_g), about -15 ^{O}C. Incorporation of a soft, elastomeric phase as a toughening agent is an effective way to improve the low-temperature impact strength of PP. Various elastomers have been used as impact modified, but EPR is the most common. The resulting PP/elastomer polymer systems are normally multiphasic, with the elastomer as the minor, dispersed component. Impact enhancement is usually achieved at the cost of a reduction in modulus and strength.

2.2.7 EPR Blends

In PP/EPR blends, the multiphasic morphology was observed by microscopy and dynamic mechanical tests [21]. In microscopic studies, three types of dispersed morphology were observed at different compositions. When EPR forms the minor phase, the average size of dispersed EPR particles depended largely on the relative viscosity between PP and EPR; the morphology of a very fine and uniform distribution of the EPR particles could be obtained when the two component polymers had similar melt viscosities. In the intermediate composition range, the blends with a lower viscosity EPR showed cocontinuous morphology in a wider range of concentration than those with higher viscosities. At high elastomer content, as expected, EPR forms the matrix and PP droplets are dispersed in it. Dynamic mechanical analysis (DMA) showed that the transition temperature of the blends were identical to the pure components, indicating total incompatibility between PP and EPR, in spite of the intimate mingling of the phases. The rules controlling the morphologies in PP/EPR blends are also to PP/EPDM systems [21].

In injection molding of these blends, two distinct morphological layers are generally observed within the cross section [3]. Near the top surface, there exists a shear zone having an elongated elastomer phase. Elastomer particles in this zone are highly stretched and oriented with the injection direction as a result of high shear rates near the wall during mold filling coupled with a high cooling rate. It is also possible that, during injection molding, some elastomer particles in the core zone are elongated by flow, and spherulites nucleate along rows due to the shear. However, the slower cooling rates of polymer melt in this region allow the elastometric inclusions time to relax, yielding spherical droplets. The morphology of the shear zone has significant effects on surface character, while the physical properties depend more on the morphology of the zone core.

The crystallization behavior of PP-based blends containing EPR or EPDM has also been reported. A substantial increase in the number of nuclei in the blends with increasing elastomer content in the system has been found [22]. The change in nucleation density was first attributed to nucleation is the result of a greater number of heterogeneous nuclei (inorganic residues and contaminants) that migrate from the EPR phase into PP during the mixing process. Using EPR copolymers with a reduced number of heterogeneities.

Although the rubber is clearly immiscible with PP, the character of the PP spherulites has been shown to be affected by the rubber addition. Melting points and heats of fusion (PP basis) were lower, and the spherulites were more irregular in texture and boundaries. At the same time, the crystallization temperatures are raised, based on the nucleation mentioned above. Unfortunately, nucleation, by raising the crystallization temperature, would work to reduce impact; smaller, but more dense and more brittle spherulites would result. Many investigators confuse this behavior observation of the less regular, lower melting spherulites in EPR/PP blends is more likely to explain the improved impact than nucleation.

In a tensile test, results obtained from a large number of blends have shown that elastic modulus is not very sensitive to structural differences [23]. In fact, its value depends almost entirely on composition and moduli of constituent components. Young's modulus of PP/elastomer systems, as expected, decreases with increasing the EPR or EPDM content [24]. Chemical modification of EPR or PP by maleic anhydride grafting did not cause any significant effect on concentration dependence of elastic modulus.

2.2.8 Additives in PP

Virgin PP directly from a commercial process is very susceptible to air oxidation. If stored unstabilized at ambient temperature, the physical properties of the product deteriorate rapidly over a period of weeks or months depending on the physical form, temperature, available oxygen, and other considerations. This

exothermic reaction can be prevented by the addition of a few parts per million of an antioxidant to the reactor product before drying and storage. This is often referred to as an in-process stabilizer [20].

Beyond the need for stabilization, additives are used in PP for the following reasons:

- Adjust color: Polypropylene is whitish in color: Pigments are used to add color to the manufactured articles. Pigments mat also have an impact on stability and physical properties.

- Alter stiffness: Polypropylene homopolymers and copolymers are typically semicrystalline materials which are manufactured to obtain various degree of stiffness. The stiffness can be further adjusted through the addition of plasticizers, nucleators, or fillers.

- Control transparency: Polypropylene is translucent. Its transparency is dramatically improved with clarifying additives. It can also be rendered opaque with pigments and fillers.

- Lower molecular weight and molecular weight distribution: Additives can be used to reduce the molecular weight and narrow the molecular weight distribution. This alters processing characteristics and physical properties.

- Decrease static buildup: Polypropylene is a natural insulator and can build static charge. Several types of additives are used as antistats.

- Control surface properties: Various additives can be used to modify the frictional and adhesion properties of PPs.

- Neutralize catalyst residues: Acid scavengers are routinely incorporated to neutralize catalyst residues and prevent equipment corrosion.

- Suppress transition metal catalyzed oxidation: The oxidation of PP is accelerated by certain metals. Several types of metal chelators successfully suppress this phenomenon.

- Enhance whiteness: Fluorescent or whitening agents are used to enhance whiteness or brilliancy of pigmented and unpigmented articles.

- Prevent biological growth: Biocides are used to prevent biological growth on the surface of PP articles.

2.2.9 Calcium carbonate-filled PP

Calcium carbonate is one of the most abundant white mineral (15%) in the earth's sedimentary crust. Although the plastic industry only accounts for about 20% of the total industrial use of calcium carbonate, carbonate is, nevertheless, the primary mineral additive or extender used in plastic. Other major make for the consumption of the carbonate include the paint, adhesive, and carpet-backing industries [25].

Calcium carbonate is filler commonly used in PP resins. It is available from a number of suppliers with chemical coating and special coupling agents designed for specific polymer systems. Additionally, various grades of calcium carbonate are produced to meet certain stringent requirements of plastic, paint and mechanical applications. Beside improvements in the purification processes, calcium carbonates are produced with mean particle size ranging 0.8 microns for finer grades to 40 micron for the coarser grades; and some have reduced particle size distributions.

The addition of calcium carbonate to polypropylene at levels ranging from 20%-40% by weight will increase the impact strength, reduce flexural modulus and mold ability. Moldable homopolymer and copolymer polypropylene generally contain finely ground carbonate of an average size 13 microns. In many polypropylene application, carbonate completes with talc, but carbonate has advantage when color, impact, or hardness is important. Surface-coated or fine

grades of calcium carbonate have better dispersion in polypropylene than do uncoated or coarse grades.

2.2.10 Kaolin-filled PP

Kaolinite is a white, nonporous, nonswelling, natural aluminosilicate mineral. In industry, it is often referred to as clay, even though physical properties greatly differ from other commercial clay silicates. Kaolin is one of the most highly refined naturally occurring minerals [25].

The primary market for kaolin in the paper industries. Kaolin also important industrial niches in plastics, rubber, fertilizer, ceramic, ink, adhesive, textile, and pharmaceutical industries. In addition to large-volume amorphous plastic, kaolin is an extensively in engineering thermoplastics. The high purity, whiteness, moderate aspect ratio, and uniformity of commercial kaolin products are all advantageous in these more demanding applications. Also, the very inert surface properties of kaolin are exceedingly important to kaolin's use in many coating and composite formulations containing a wide variety of other chemical additives. Commercial materials from domestic sources usually have an aspect ratio of around 6:1. The very coarse fractions from kaolin deposits usually contain large particles that are long curled stacks of hexagonal plates.

Kaolin is extensively used in polyolefin (as well as in rubber and plastic) applications requiring good electrical properties. Surface-treated grades are used in cross-linked polyethylene wire insulation to improve not only the electrical properties, but also tensile strength, cut-through resistance, and processing. The surface treatment also prevents the acidic kaolin surface from degrading the peroxide curing catalysts.

2.2.11 Crystallization behavior

Polypropylene is a semi-crystalline polymer. Its properties are determined by its crystalline structure and the relative amount of amorphous and crystalline phases, crystal structure, size and perfection of crystallites, dimensions of spherulites and the number of tie molecule. The crystalline phase of polymers consists of thin plates or ribbons with the chains oriented along the thin dimension. The amorphous region consists of chain-end cilia, totally occluded chains, and chains which are incorporated into two or more crystals (tie chains). The tie chains determine the mechanical continuity of the system and thereby control the elastic modulus as well as yield strength.

The higher cystallinity of the PP with coarse spherulitic structure leads to a larger volume contraction and thus to formation of voids and micro cracks. Consequently, the crack path tends to follow the weak spherulite boundaries, resulting in a very low fracture toughness value.

In general, it is believed that the spherulitic nucleation takes place at heterogeneities in the melt such as catalyst residues, dust particle low-molecular weight fractions, branch points, stereo-irregular molecules, fillers or specific nucleating agents. The spherulite size is primarily dictated by the volumetric nucleation rate, which depends on thermal history, nature of the surface and degree of undercooling. The amount of crystallinity and spherulite size influences the modulus and strength of PP. Spherulite size and spherulite boundaries significantly influences the yield and the failure behavior of polymers. These effects are manifested in the macroscopic nature of the fracture path.

The fine spherulite microstructure produced by adding nucleating agents gives rise to greatly enhanced ductility, yield strength, and impact strength. In general, refinement of the spherulite size by either homogeneous or heterogeneous nucleation, or by reducing the crystallization temperature results in improved ductility an strength.

It is clear that the large spherulite exhibits cracks at spherulite boundaries, whereas systems with smaller spherulite draw smoothly.

2.3 Literature reviews

Tjong S.C. et el. [26] investigated calcium carbonate fillers on β crystalline phase polypropylene composites. Thus the incorporation of the calcium carbonate filler into the β-iPP matrix generally. The addition of the fillers reduces amount of the β- phase content static tensile measurements showed that the elastic modulus of the composites increase with the increasing filler content but the yield strength decrease. The decreasing yield stress of particulated filler thermoplastics is due to cracking and splitting of aggregated particles. The facture impact toughness with increasing filler content is attributed to decrease in the concentration of the tougher polymer matrix, an increase in the amount of the weaker filler/matrix interface, and to the debonding of the filler from the polymer matrix.

Varga J. et al. [27] reported that calcium salts of pimelic and suburic acids are highly active, thermally stable β-nucleating agents. Isotactic homopolymers and random and block copolymers of polypropylene crystallize almost purely in β modification, even at a low concentration. Ca-Sub proved to be the most effective β-nucleating agent found iPP crystallized in pure β form up to a temperature of ~140°C. These additives caused significant changes in crystallization, melting characteristics, and structure of the polymers. The degree of crystallinity of the β-nucleated samples was markedly higher than that of the α-modification. Similar features were found the melting behavior of α- and β-iPP crystallized isothermally in a wide temperature range.

Li X. et al. [28] reported that the effect of seven dicarboxylates of calcium on the formation of β-form polypropylene. Calcium pimelate, calcium suburate, calcium phthalate and calcium terephthalate have found to be an effective β nucleators. Calcium succinate, calcium adipate, and calcium sebacate behave invalidly on the nucleating of the β phase. The effective nucleators reveals a common character that their first reflection locate at the d-spacing between 10 to 13°A, indicating structural similarity of the nucleators with β iPP.

Sterzynski T. et al. [29] also observed that the linear trans-quinacridone dye as β phase nucleator and a dimethyl quinacridone resulting in formation of pure α phase structure. A maximum of the k value that fraction of β phase was found for a concentration of 5 x 10^{-5} wt% of the trans-quinacridone. DSC giving a characteristic double melting peak for the β polypropylene ,indicating melting at 148 ^{O}C of the metastable β phase and when increase for both nucleating agents, the crystallization temperature (T_{cr}) was increase with higher T_{cr} value for α nucleated iPP. They reported that the α phase iPP show a higher modulus than β iPP and increasing nucleating agents concentration the modulus increase. For the β phase iPP the highest value of the k parameter . On the SEM observation, which permitted the detection of spherulites with cross-hatched lamellae for the α spherulites and with simple radial growth lamellae for β spherulites.

Feng J. et al. [30] investigated nineteen kinds of minerals, alone and bicomponent mixtures with a mixed ternary complex of trivalent lanthanum sterate and sterin (LaC) , were added to isotactic polypropylene. A wide angle X-ray diffraction examination demonstrated that no mineral or LaC acting alone could induce β form, whether the calcium compound has a hexagonal crystallographic form or not. They surmise that the actual β iPP substrate in such a system might be some binuclear complexes of calcium and rare earth elements with same specific ligands.

Chan C. et al. [31] reported that the tensile modulus of PP composites with $CaCO_3$ nanocomposites increased by approximately 85 % while yield stress and strain were not much affected by the presence of $CaCO_3$ nanocomposites. The studies showed that the nanocomposites were distributed in PP matrix uniformly and little particles agglomeration was found at 4.8 and 9.2 %. Thermal analysis and SEM studies on PP and nanocomposites revealed that the $CaCO_3$ nanocomposites are the effective nucleating agent that the causes the absence of detectable spherulites. And the incorporation of $CaCO_3$ nanocomposites in PP has significantly increased its impact strength by approximately 300%.

Todjeman Ph. et al. [32] studies the effect of the α and β crystalline structure of polypropylene on its mechanical properties. Young modulus and yield stress reduce slowly with an increase in β phase content and the fracture toughness of PP increases greatly with its β phase content. They reported that the occurrence of tangential lamellae in the α phase makes the spherulites more rigid and causes increase in Young modulus and yield stress with the α phase content and these tangential lamellae restrict the elongation at break of the spherulites and make the PP more bittle.

Li Y. et al. [33] reported that polypropylene filling 4-6 vol % of $CaCO_3$ nanoparticles, the strength of PP can be optimally enhanced. As the content of nm-$CaCO_3$ particles further increase, the number of β crystals nuclei will increase, thus the size of β crystals would decrease, which may cause the decrease in strength of composites sample. Around 4 vol% nm- $CaCO_3$ particles, the activation energy and the peak temperature of α phase exhibit minimum and maximum values respectively.

CHAPTER III

EXPERIMENTAL

3.1 Materials

1. Heterophasic copolymer or PP/EPR blends (Moplen EP300L) supplied by HMC Polymers CO., Ltd., Rayong, Thailand. MFI loaded by 2.16 kg at 230 ^{O}C of 0.5 g/10 min and density of 0.905 g/cm^3.

2. Pimelic acid (Heptanedioic acid ; $C_7H_{12}O_4$) supplied by MERCK KcaA, Germany.

3. Suberic acid (Octanedioic acid ; $C_8H_{12}O_4$) supplied by MERCK KcaA, Germany.

4. Calcium sterate supplied by Imperial Industrial Chemical.

5. Calcium carbonate, average particle size 0.8 μm supplied by Usrint Chemical (Thailand) Ltd.

6. Calcium carbonate, average particle size 40 nm supplied by NanoMaterials Technology Pte Ltd.

7. Kaolin (SATINTONE 5 HB), average particle size 0.8 μm, U.S.A. supplied by Centasia Co., Ltd.

3.2 Instruments

Major instruments were used and listed below

1. LTE 26-40 system twin screw extruder (LAB TECH Engineering Co., Ltd., Thailand).

2. LZ-120 /VS Pelletizing unit (LAB TECH Engineering Co., Ltd., Thailand).

3. Injecting Molding Machine model Arburg allrounder ® 270 m.

4. HOUNSFIELD universal testing machine.

5. Pendulum 4 J Model 6545 Izod impact tester.

6. CEAST Model 6525 Notching machine.

7. Metter Toledo Model DSC 822 Differential scanning colorimeter.

8. JEOL JDX-3530 X-ray diffactometer.

9. Polarizing Microscope LEICA DM RXP.

3.3 Experimentals

3.3.1 Preparation of nucleating agent on β-phase of PP/EPR blend

In this study, two types of nucleating agents were firstly blended with PP/EPR blend for selection one type which shown higher in β-phase. These blends were prepared as 3 formulas;

1. PP/EPR blended without β-nucleator control

2. PP/EPR blended filled with 0.001 wt.% of Ca-Pim

3. PP/EPR blended filled with 0.001 wt.% of Ca-Sub

Each formulation was melt-mixed in twin screw extruder at 190/200/210/220 ^{O}C (from hopper to nozzle), 95 rpm and then palletized with granulator. These pallet samples were molded to form dumbbell shape specimen and impact specimen for mechanical testing by injection molding machine at 150/160/170/180/190 ^{O}C (from hopper to nozzle).

3.3.2 Preparation of filler filled to PP/EPR blend

The PP/EPR blends were thoroughly dry mixing with and without added two types of fillers; kaolin (K) and $CaCO_3$(C) were prepared to form mechanical testing samples the same as section 3.3.1. The formulas of these blends in Table 3.1

Table 3.1 The formulation of PP/EPR blends with and without fillers

Sample code	Filler added (wt.%)	
	Kaolin	$CaCO_3$
PN_0K_1	5	-
PN_0K_2	10	-
PN_0K_3	15	-
PN_0C_1	-	5
PN_0C_2	-	10
PN_0C_3	-	15

3.3.3 Preparation of filler filled with and without β-nucleator to PP/EPR blends

The blends of PP/EPR added with and without added β-nucleator; pimelic acid and calcium stearate (N_1), and fillers; μm-$CaCO_3$(C), and nano$CaCO_3$ (Cn) were prepared to form mechanical testing samples the same as section 3.3.1. The formulas of these blends shown in Table 3.2.

Table 3.2 The formulation filler filled with and without β-nucleator to PP/EPR blend

Sample code	Nucleator added (wt.%); Ca-Pim	Filler added (wt.%)	
		CaCO$_3$	Nano-CaCO$_3$
PN$_1$C$_1$	0.001	5	-
PN$_1$C$_2$	0.001	10	-
PN$_1$C$_3$	0.001	15	-
PN$_1$Cn$_1$	0.001	-	5
PN$_1$Cn$_2$	0.001	-	10
PN$_1$Cn$_3$	0.001	-	15

3.3.4 Preparation of crystallized with PP/EPR composites.

The pellet sample from extrusion process filled with and without added β-nucleator; pimelic acid and calcium stearate (N$_1$), and fillers; μm-CaCO$_3$(C), and nanoCaCO$_3$ (C$_n$) (3.3.3) were compressed to form thinning plate by thinning compression mold plate, melted in hot state from 40 ^{O}C to 220 ^{O}C, 5 minutes, and crystallized with isothermal temperature at 130 ^{O}C, 30 minutes.

3.4 Characterization and measurements

3.4.1 Mechanical properties

3.4.1.1 Determination of tensile properties

The dumbbell shaped specimens which molded from injection machine (from 3.3.1-3.3.3) were measured following the procedures described in ASTM D638 method A using universal testing machine, computer controlled measurement system.

The tensile parameters and testing condition, speeding testing of 50 mm/min, gauge length of 50 mm, load cell of 50 Kg$_f$ and temperature $23\pm 2^{\circ}C$ were used. The measurement of tensile strength at yield (MPa), elongation at yield (%) and modulus (MPa) were made with six specimens in each blends.

3.4.1.2 Determination of flexural modulus

The dumbbell shaped specimens which molded from injection machine (from section 3.3.1-3.3.3) were performed with ASTM D790 method A using universal testing machine, which computer controlled measurement system, three point loading system with diameter of support rods and loading rod 4 and 10 mm, respectively. The condition of testing specimens was set at $23\pm 2^{\circ}C$ and 50 ± 5 % humidity for not less 40 hrs prior to the test accordance with method A. The flexural modulus (MPa) was measured with six specimens in each blends.
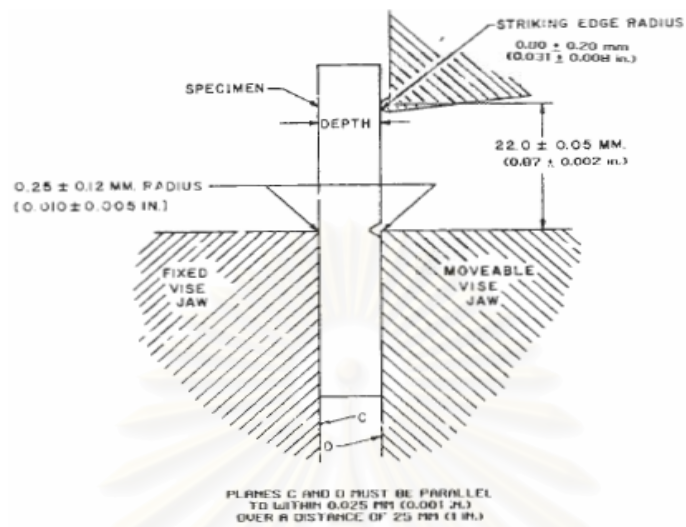
Figure 3.1 Relationship of vise, specimen, and striking edge to each other for Izod test method A and C.
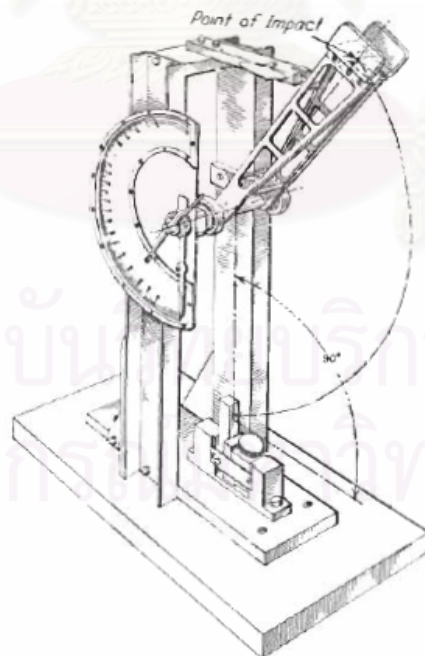
Figure 3.2 Cantilever beam (Izod-type) impact machine

3.4.1.3 Determination of impact strength

The impact test specimen with dimension of 6.35 by 1.27 by 0.64 cm and 0.0254 cm of notched radius (from injection molded in section 3.3.1-3.3.3) with six specimens in each blend was accomplished on PENDULUM 25J Izod impact tester. The test procedure conformed to the ASTM D256 method A. Each specimen was held as a vertical cantilever beam and broken by a single swing of the pendulum with the line of initial contact at a fixed distance from the specimen clamp and from the centerline of the notch and on the same face as the notch. The line of contact of the striking nose is located at the center of percussion of the pendulum within ± 2.54 mm. (0.10 in). Store the test specimens at 23 ± 2 ^{O}C and 50 ± 5 % humidity for not less 40 hrs after notching and prior to measuring.

3.4.2 Thermal analysis

The test specimens which molded from injection machine (from 3.3.1-3.3.3) and crystallized at 130°C (3.3.4) were measured the melting temperature (T_m) and crystallization temperature (T_c) by using a Metter Toledo Model DSC 822. Indium and zinc standard were used for temperature calibration. This samples cut from the specimens weighing about 5 mg were put into a DSC sample pan and melted in a furnace in nitrogen atmosphere from 40°C to 220°C at a heating rate of 20°C/min following by 20°C/ min cooling. T_m and T_c were determined during the cooling and the second heating. The peak temperature of the exothermic curve was taken as T_c , whereas the endothermic curve was T_m.

3.4.3 X-ray diffraction measurement

The specimens were prepared from injection-molded bars, of which their outer skin was carefully removed by a very fine sandpaper (from 3.3.1-3.3.3) and the pallet sample from extrusion process was compressed to form thinning plate by thinning compression mold plate and crystallization with isothermal temperature at 130°C (3.3.4) then measured the x-ray diffraction patterns using the x-ray diffractometer. Nickel-filtered CuK$_\alpha$ radiation ($\lambda = 0.154187$ nm) operated at 50 kV and 30 mA was employed. The patterns were recorded with the incident X-ray beam

positioned at the angle $2\theta = 10\text{-}40$ degrees to the test specimen surface. This technique is generally used to investigate the crystal structure. The K value corresponding to the relative amount of the β-form was calculated using following formular

$$K = \frac{H_\beta(300)}{H_\beta(300) + H_\alpha(110) + H_\alpha(040) + H_\alpha(130)}$$

Where $H_\alpha(110)$, $H_\alpha(040)$, and $H_\alpha(130)$ are the intensities of the X-ray diffraction of the α-reflection and $H_\beta(300)$ is the intensity of the reflection measured as the height of the peaks. The K- value tends to zero if no β-form is present and to unity in the case when a lot of β-form is also present.

3.4.4 Spherulitic structure study of β-form PP samples

The pallet sample from extrusion process was compressed to form thinning plate by thinning compression mold plate and crystallization with isothermal temperature at $130^\circ C$ (3.3.4), and spherulitic structure was studied by Polarizing Microscope LEICA DM RXP.

CHAPTER IV

RESULTS AND DISCUSSION

4.1 Effect of nucleating agents on β-phase of PP/EPR blend

It is generally known that polypropylene (PP) can crystallize more than one crystalline form, i.e. α and β forms. Its prevalent form depends on the nucleating agent type added. The most effective β-nucleating agent for polypropylene is the calcium salt of pimelic acid (Ca-Pim) [14,26,27,28]. The other known nucleating agent is the calcium salt of suberic acid (Ca-Sub) [14,27,28,36]. Kessaraporn [34] reported that Ca-Pim filled- PP/EPR blend at 0.001 wt.% as a thin film had highest K-value is 0.75.

In this work, it is to investigate the effect of both nucleating agents on β-phase and mechanical properties of PP/EPR blend. Figure 4.1 shows the WAXD diagrams of PP/EPR blend samples filled with and without 0.001 wt.% Ca-Pim or 0.001 wt.% Ca-Sub. The specimens were prepared from injection-molded bars, of which their outer skin was carefully removed by a very fine sandpaper. The relative amount of the β-phase content (defined as "K-value") in these specimens can be calculated by the Turner-Jones equation. The calculated K-value of neat PP/EPR blend (PN_0) and PP/EPR blend samples filled with 0.001 wt.% Ca-Pim (PN_1) and 0.001 wt.% Ca-Sub (PN_2) was 0, 0.24, and 0, respectively.
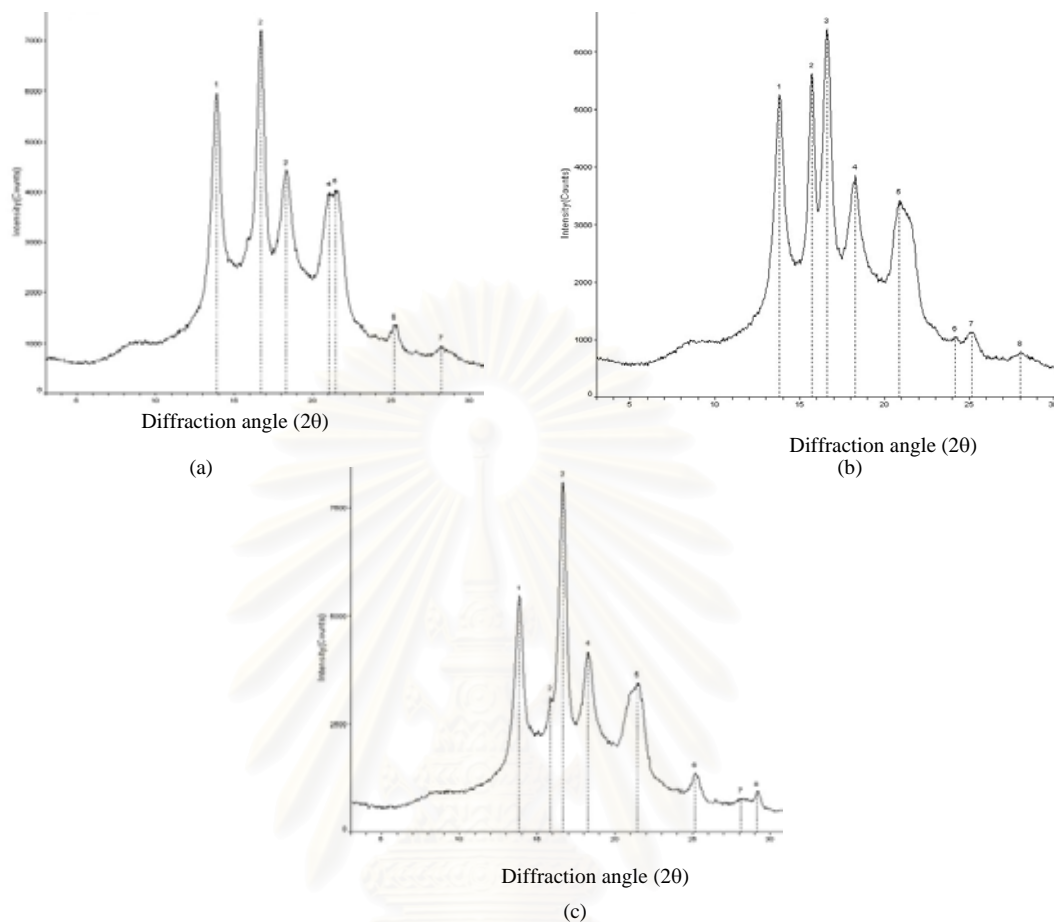
Figure 4.1. WAXD diagrams of neat PP/EPR blends (a),PP/EPR blend filled with 0.001 wt.% Ca-Pim (b) and PP/EPR blend filled with 0.001 wt.% Ca-Sub (c).

Table 4.1 β-phase index (defined as K-value) of PP/EPR blend and PP/EPR blend filled with nucleator.

Sample code	Nucleator (wt.%)		H_β	$H_{\alpha1}$	$H_{\alpha2}$	$H_{\alpha3}$	K-value
	Ca-Pim	Ca-Sub					
PN_0	-	-	0	3789	4433	1758	0
PN_1	0.001	-	2619	3272	3448	1540	0.24
PN_2	-	0.001	0	3551	5595	1791	0

Note : $H_{\alpha1}$, $H_{\alpha2}$, $H_{\alpha3}$ are intensities of α-diffraction peaks corresponding to angle θ = 7.1^O, 8.5^O, and 9.4^O, and $H_{\beta1}$ is the intensity of β-diffraction peaks corresponding to angle θ = 8.1^O

There was no β-peak occurrence in WAXD diagram for unfilled PP/EPR blend and PP/ERR blend filled with 0.001 wt% Ca-Sub, the amount of β-crystalline form when 0.001 wt% Ca-Pim added, indicated as k-value of 0.24. Li. et al. [28] reported that Ca-Sub 0.5 wt% could promoted β-crystalline, indicated as k-value of 0.96 in isotactic polypropylene. It is well known that the disturbance of regularity of the polymer chain reduces the tendency for β-crystalline in random copolymer [36], therefore in this result, the concentration of β-nucleating agent (Ca-Sub) was too low to promote β-crystalline in this copolymer. Ca-Pim filled system was the result of the formation of the β-phase in PP/EPR blend, further investigations will be conducted in order to verify the hypothesis drawn.

In this study Ca-Pim is more effective nucleating agent than Ca-Sub was same content, then it is interesting to investigate further.

4.2 Addition of fillers in PP/EPR blend

4.2.1 Effect of fillers on mechanical properties of PP/EPR blend

It is well known that mineral fillers improve the rigidity of the polymers. Indeed, most of the fillers, especially calcium carbonate and kaolin, have been used to fulfill various industrial functions, e.g. upgrading flexural modulus or tensile modulus of the final products. Kessaraporn [34] reported that flexural modulus of talc filled-PP/EPR blend at loading 30 and 40 wt. % was more than twice as much as unfilled-PP/EPR blend and the tensile strength value was not significantly difference between filled and unfilled composite in same loading. Then, it is interesting to investigate further whether calcium carbonate and kaolin influence the mechanical properties of PP/EPR blend in other loading (5, 10, 15 wt.%) to improve both flexural modulus or tensile modulus.

Table 4.2 shows mechanical properties of PP/EPR blend (PN_0) filled with kaolin (K), and calcium carbonate micro-particles (C).

Table 4.2 Mechanical properties of PP/EPR blends filled with kaolin and calcium carbonate

Sample code	fillers (wt.%)		Tensile Strength (MPa)	Elongation at Yield (%)	Tensile Modulus (MPa)	Flexural Modulus (MPa)	Izod Impact Strength (J/m)
	kaolin	μm-CaCO$_3$					
PN$_0$	0	0	22.1 $\pm$ 0.2	6.7 $\pm$ 0.1	713.5 $\pm$ 4.8	1002.3 $\pm$ 9.2	149.7 $\pm$ 6.3
PN$_0$K$_1$	5	0	22.8 $\pm$ 0.0	6.2 $\pm$ 0.1	1117.2 $\pm$ 7.4	1054.5 $\pm$ 6.2	443.4 $\pm$ 9.5
PN$_0$K$_2$	10	0	22.3 $\pm$ 0.2	5.5 $\pm$ 0.1	1211.8 $\pm$ 5.0	1179.5 $\pm$ 6.5	307.0 $\pm$ 10.0
PN$_0$K$_3$	15	0	19.4 $\pm$ 0.1	5.5 $\pm$ 0.1	1186.5 $\pm$ 6.5	1258.5 $\pm$ 9.2	251.2 $\pm$ 4.9
PN$_0$C$_1$	0	5	20.3 $\pm$ 0.6	6.9 $\pm$ 0.1	1145.8 $\pm$ 4.5	1031.7 $\pm$ 6.7	440.0 $\pm$ 9.0
PN$_0$C$_2$	0	10	20.5 $\pm$ 0.3	6.9 $\pm$ 0.1	1209.3 $\pm$ 5.7	1136.7 $\pm$ 5.5	224.5 $\pm$ 2.8
PN$_0$C$_3$	0	15	19.2 $\pm$ 0.2	5.2 $\pm$ 0.1	1279.7 $\pm$ 8.7	1248.7 $\pm$ 4.9	195.8 $\pm$ 5.0

According to Table 4.2, the tensile strength and elongation at break and were not significantly different between filled and unfilled composites. The tensile modulus of kaolin- and μm-CaCO$_3$–filled PP/EPR blend are higher than unfilled PP/EPR blend and the highest value was observed for the sample filled with 15 wt.% μm-CaCO$_3$ (PN$_0$C$_3$). Li. et al. [35] reported that the decrease in the yield strength of particulate-filled thermoplastics is due to cracking and splitting of aggregated particles. It should be noted that the dispersion of the fillers in the polymer matrix is not perfect, e.g., the filler tends to aggregate. The adhesion between the aggregates and the polymer matrix is known to be very poor. If there is breaking of aggregates, the yield strength tends to decrease with increasing the filler content. When the surface of the fillers is treated or coupling agent is used, the adhesion between the fillers and the polymer matrix could be improved. In

this case, a stronger filler-matrix interface can be produced and the applied load is efficiently transferred to the filler thereby increasing the yield strength. Somehow, the results showed that the impact strength of both kaolin (PN_0K_1) and μm-$CaCO_3$ (PN_0C_1)–filled PP/EPR blend at 5 wt.% loading was about three times as much as that of the unfilled PP/EPR blend and it decreased with increasing the filler content. The increase in the impact resistance at the low filler contents may be attributed to the formation of the smaller crystallites, as well as to the ability to absorb more energy by amorphous phase. The main reason for the decrease in impact resistance with increase fillers contents are likely the poor adhesion at the polymer matrix and fillers.

4.2.2 Effect of fillers on β-phase formation in PP/EPR blend

From above investigation, kaolin and μm-$CaCO_3$ could improve mechanical properties of PP/EPR blend, especially in the cases of tensile modulus, flexural modulus and impact strength. It is interesting to investigate further whether kaolin and μm-$CaCO_3$ influences the formation of α-crystalline or β-crystalline form. Figure 4.2 shows the WAXD diagrams of kaolin-filled and μm-$CaCO_3$-filled PP/EPR blend in various filler loadings (i.e. 5, 10, and 15 wt.%). These samples were prepared by injection molding and the outer skin layer was carefully removed by way of abrasion with very fine sandpapers.

(a)

(b)

(c)

(d)

(e)

(f)
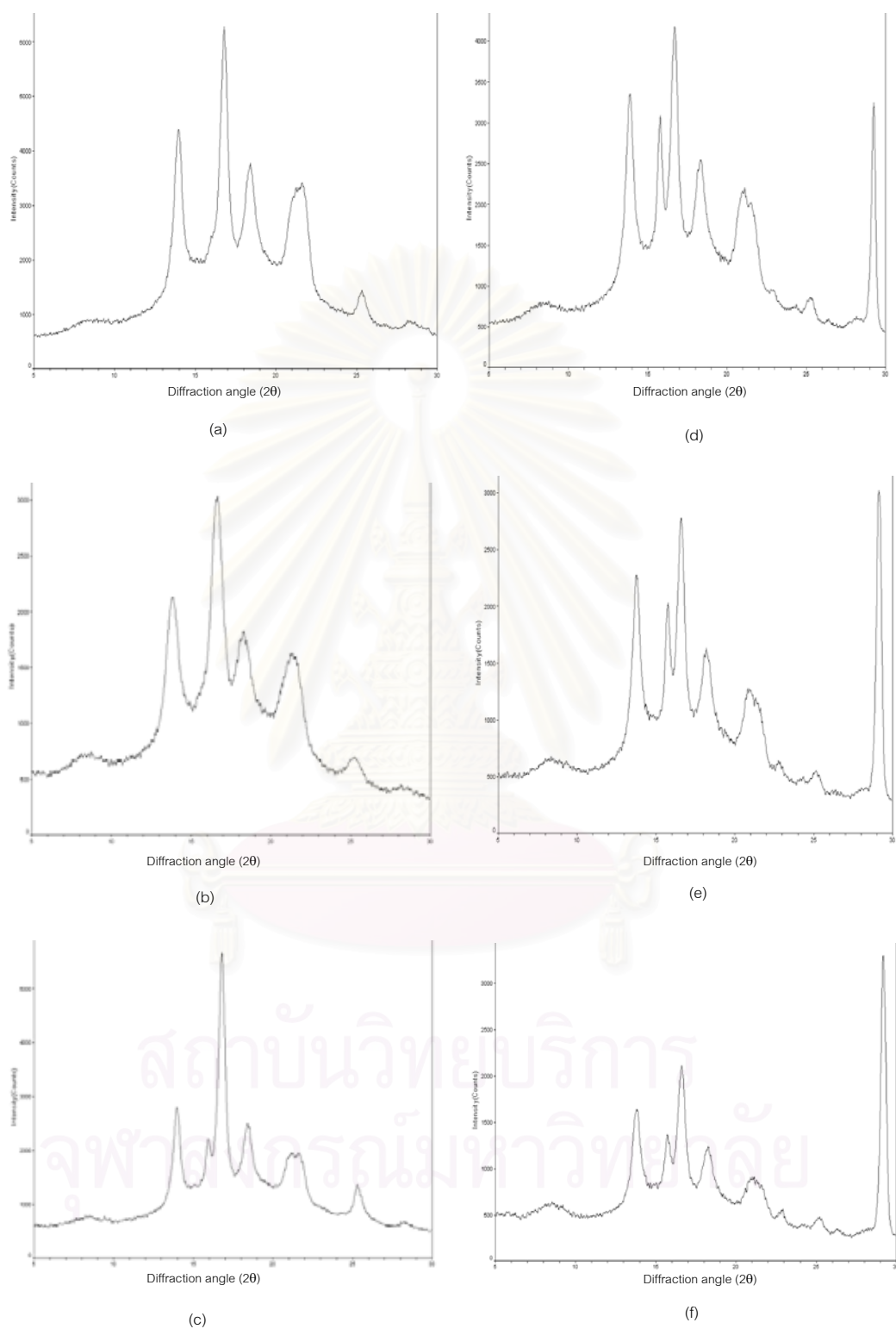
Figure 4.2 WAXD diagrams of kaolin-filled PP/EPR blend containing 5 (a), 10 (b), 15 wt.% (c) and μm-CaCO$_3$-filled PP/EPR blend containing 5 (d), 10 (e), and 15 wt.%(f).

Table 4.3 K-value of kaolin-filled PP/EPR blend containing 5 , 10 , 15 wt.% and μm-
$CaCO_3$-filled PP/EPR blend containing 5 , 10 , and 15 wt.%.

Sample code	kaolin (wt.%)	$CaCO_3(\mu m)$ (wt.%)	H_β	$H_{\alpha 1}$	$H_{\alpha 2}$	$H_{\alpha 3}$	K-value
PN_0K_1	5	0	0	4397	6287	3774	0
PN_0K_2	10	0	0	2130	3037	1823	0
PN_0K_3	15	0	2201	2784	5673	2491	0.17
PN_0C_1	0	5	3089	3352	4181	2545	0.23
PN_0C_2	0	10	2031	2279	2776	1628	0.23
PN_0C_3	0	15	1363	1641	2118	1234	0.21

Note : $H_{\alpha 1}$, $H_{\alpha 2}$, $H_{\alpha 3}$ are intensities of α-diffraction peaks corresponding to angle $\theta = 7.1^O$, 8.5^O, and 9.4^O, and $H_{\beta 1}$ is the
intensity of β-diffraction peaks corresponding to angle $\theta = 8.1^O$

From Figure 4.2 and Table 4.3, there was no β-peak occurred in the
WAXD diagrams of PN_0K_1 and PN_0K_2, which were the samples filled with kaolin
at 5 and 10 wt.%. However, when the kaolin content increased to 15 wt.% (K-
value = 0.17), β-phase was observed by WAXD diagram. Besides, β-form
expressed in WAXD diagrams of PN_0C_1, PN_0C_2 , and PN_0C_3 samples which were
the samples filled with 5, 10, and 15 wt.% μm-$CaCO_3$. The corresponding K-
values were 0.23, 0.23, and 0.21, respectively (see Table 4.3). Based on these
results, it appears that μm-$CaCO_3$ can act as both filler and β-nucleator better than
kaolin. Because of a face spacing of μm-$CaCO_3$ is able to serve as effective
nucleating agent (11-13 Å). It is interesting to investigate further in case of $CaCO_3$
filled with nucleating agent.

4.3 Addition of Ca-Pim and calcium carbonate in PP/EPR blend

In the previous section, it was found that $CaCO_3$ microparticles promoted the formation of β-phase in PP/EPR blend better than kaolin. It should therefore be very interesting to see if it is possible to improve flexural modulus, tensile modulus, and Izod impact strength at the same time by loading both $CaCO_3$ and Ca-Pim into PP/EPR blend. At the same time, it is also interesting to study the effect of $CaCO_3$ particle sizes (i.e. micrometer and nanometer range) on the mechanical properties of the filled samples. These samples were subjected β-phase measurement, mechanical property testing, and thermal analysis.

4.3.1 Mechanical properties

Specimens used in study were prepared by blending 0.001 wt.% Ca-Pim and $CaCO_3$ with PP/EPR blend at various loadings. The mechanical properties are summarized in Table 4.4.

Table 4.4 Mechanical properties of Ca-Pim and calcium carbonate in PP/EPR blend

Sample code	Nucleator content (wt.%)			Tensile Strength	Elongation at Yield	Tensile Modulus	Flexural Modulus	Izod Impact Strength
	Ca-Pim	$CaCO_3$ (μm)	$CaCO_3$ (nm)	(MPa)	(%)	(MPa)	(MPa)	(J/m)
PN_0	0	0	0	22.1 ± 0.2	6.7 ± 0.1	$713.5 \pm 4.$	1002.3 ± 9.2	149.6 ± 6.3
PN_1	0.001	0	0	21.3 ± 0.2	7.8 ± 0.1	1050.2 ± 7.3	915.3 ± 8.6	511.0 ± 5.3
PN_1C_1	0.001	5	0	19.9 ± 0.3	7.8 ± 0.1	1107.5 ± 4.0	1001.5 ± 8.6	287.9 ± 3.5
PN_1C_2	0.001	10	0	19.2 ± 0.2	7.7 ± 0.1	1122.7 ± 4.1	1179.2 ± 4.4	254.7 ± 8.7
PN_1C_3	0.001	15	0	17.7 ± 0.2	5.2 ± 0.0	1192.0 ± 5.6	1231.0 ± 4.2	221.9 ± 8.4
PN_1Cn_1	0.001	0	5	20.4 ± 0.3	6.9 ± 0.1	1001.5 ± 8.6	1023.7 ± 8.2	511.6 ± 8.8
PN_1Cn_2	0.001	0	10	19.3 ± 0.3	7.8 ± 0.0	1179.2 ± 4.4	1006.2 ± 3.8	456.9 ± 9.0
PN_1Cn_3	0.001	0	15	18.2 ± 0.3	5.3 ± 0.1	1231.0 ± 7.2	1105.5 ± 9.6	101.4 ± 5.2

According to Table 4.4, the impact strength of Ca-Pim and nm-$CaCO_3$-filled PP/EPR blend at the nm-$CaCO_3$ loading of 5 wt.% (PN_1Cn_1 sample) was about four times that of the unfilled sample and the value was about the same as that of the sample filled with 0.001 wt.% Ca-Pim (PN_1 sample). Interestingly, both the tensile and the flexural moduli of PN_1Cn_1 sample were greater than that of PN_1 sample and the neat PP/EPR blend sample (PN_0 sample). In both types of fillers investigated, both the tensile and the Izod impact strength decreased, while both the tensile and the flexural modulus generally increased, with increasing the filler content. This is in good agreement with Li Y. [29] who reported that, for polypropylene filled with 4-6 vol.% $CaCO_3$ nanoparticles, the tensile strength increased at first, reached a maximum of about 35.2 MPa at 4 vol.%, and

decreased with further increase in the filler content. He attributed the occurrence to the increase in the number of β nuclei that decreased the size of β crystals, hence the observed decrease in the strength of the resulting composites.

4.3.2 β-phase formation

To quantify the amount of β-phase, the outer surface of injection-molded samples was carefully removed by abrasion. Figure 4.3 shows WAXD diagrams of PN_1C_1, PN_1C_2, and PN_1C_3 samples that contained 0.001 wt.% Ca-Pim and 5, 10, or 15 wt.% μm-$CaCO_3$ and PN_1Cn_1, PN_1Cn_2, and PN_1Cn_3 samples that contained 0.001 wt.% Ca-Pim and 5, 10, or 15 wt.% nm-$CaCO_3$. The calculated K-value are listed in Table 4.5. The X-ray diffraction analyses indicated that the formation of the β-phase was the greatest at the filler content of 10 wt.%.

From Table 4.5, the K-value of the PP/EPR blend samples filled with 0.001 wt.% of Ca-Pim and 10 wt.% of both $CaCO_3$ micro- and nanoparticles was the greatest, and in comparison with results shown in Table 4.3, addition of Ca-Pim actually increased the possibility for the formation of the β-phase. The results implied that both Ca-Pim and $CaCO_3$ particles (especially nanosized ones) helped promote the formation of the β-phase.

Figure 4.3 The WAXD diagrams of 0.001 wt.% Ca-Pim, and μm- CaCO₃ containing 5 (a), 10 (b) and 15 wt.% (c) and 0.001 wt.% Ca-Pim, and nm- CaCO₃ containing 5 (d), 10 (e) and 15 wt.% (f)- filled PP/EPR blend.

Table 4.5 K-value of composite containing 0.001 wt. % Ca-Pim, and $CaCO_3$ (μm and nm) content 5, 10 and 15 wt. %

Sample code	Ca-Pim (wt.%)	$CaCO_3(\mu m)$ (wt.%)	$CaCO_3(nm)$ (wt.%)	H_β	$H_{\alpha 1}$	$H_{\alpha 2}$	$H_{\alpha 3}$	K-value
PN_1C_1	0.001	5	0	3526	2720	3851	1313	0.31
PN_1C_2	0.001	10	0	2720	1899	2167	824	0.36
PN_1C_3	0.001	15	0	1368	1297	1531	572	0.29
PN_1Cn_1	0.001	0	5	2443	3049	5113	1540	0.20
PN_1Cn_2	0.001	0	10	2514	1844	2482	848	0.33
PN_1Cn_3	0.001	0	15	643	1448	2584	837	0.12

Note : $H_{\alpha 1}$, $H_{\alpha 2}$, $H_{\alpha 3}$ **are intensities of** α**-diffraction peaks corresponding to angle** $\theta = 7.1^O, 8.5^O$**, and** 9.4^O**, and** $H_{\beta 1}$ **is the intensity of** β**-diffraction peaks corresponding to angle** $\theta = 8.1^O$

4.3.3 Thermal properties

In this study, DSC was used to observe the melting behavior of injection-molded samples. Normally, PP in its α-phase usually melts in the range of 161-164°C. Other research reported that the melting peak of PP in its β-form was observed at 148°C, while the endothermic peak at 160°C is due to the melting of α-phase [7]. DSC is also used to identify the existence of β-crystalline form in both neat and filled PP/EPR blend samples. Figure 4.4 shows DSC traces of PP/EPR blend samples filled with 0.001 wt.% Ca-Pim and $CaCO_3$ micro- and nanoparticles as well as of PP/EPR blend sample filled with 0.001 wt.% Ca-Sub.

Only one melting peak at 164.2°C was observed for unfilled PP/EPR blend sample (i.e. PN_0 sample) and Ca-Sub-filled PP/EPR blend sample (i.e. PN_2 sample). For PP/EPR blend sample filled with 0.001 wt.% Ca-Pim (i.e. PN_1

sample), two melting peaks at 152.1 and 168.8°C were observed. This observation clearly confirmed that the existence of both the α- and the β-crystalline forms for PN_1 sample. For PP/EPR blend sample filled with 0.001 wt.% Ca-Pim and $CaCO_3$ in various amounts, two melting peaks can be found at the ranges of 150-153 and 168-169°C, respectively. Obviously, the melting peak associated with the β-crystalline structure was observed in these samples and were seen to have less of α-form and gradually exhibited the position of β-form instead.
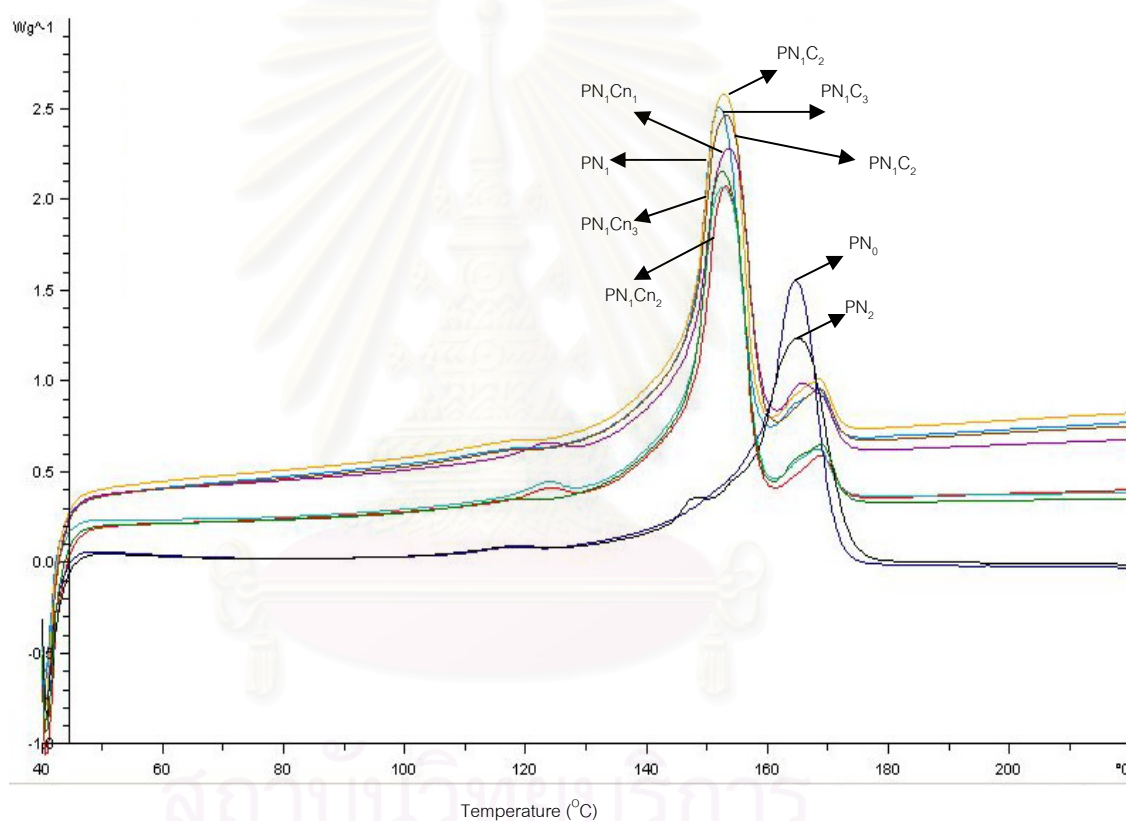
Figure 4.4 DSC traces of unfilled PP/EPR blends, Ca-Sub filled PP/EPR blend and Ca-Pim and $CaCO_3$ (μm and nm) filled PP/EPR blend.

Table 4.6 The melting characteristics of unfilled PP/EPR blend, Ca-Pim filled PP/EPR blend, Ca-Sub filled PP/EPR blend and Ca-Pim and $CaCO_3$ (μm and nm) filled PP/EPR blend

Sample	Nucleating agent (wt. %)		Filler (wt. %)		T_m (β) (^{o}C)	T_m (α) (^{o}C)	K-value
	Ca-Pim	Ca-Sub	$CaCO_3$ (μm)	$CaCO_3$ (n)			
PN_0	-	-	-	-	-	164.2	0
PN_1	0.001	-	-	-	152.1	168.8	0.24
PN_2	-	0.001	-	-	-	164.2	0
PN_1C_1	0.001	-	5	-	152.4	168.4	0.31
PN_1C_2	0.001	-	10	-	152.0	168.4	0.36
PN_1C_3	0.001	-	15	-	151.4	168.1	0.29
PN_1Cn_1	0.001	-	-	5	153.1	166.1	0.20
PN_1Cn_2	0.001	-	-	10	152.1	168.5	0.33
PN_1Cn_3	0.001	-	-	15	152.5	168.8	0.12

4.4 Determination of β-phase in isothermally-crystallized PP/EPR film samples filled with Ca-Pim and $CaCO_3$ micro- and nanoparticles

The compression-molded film samples filled with Ca-Pim and $CaCO_3$ micro- and nanoparticles were prepared at an isothermal temperature of 130°C in order to investigate the amount of β-phase formed in these samples. Figure 4.5 shows WAXD diagrams of the neat PP/EPR blend film sample (i.e. PN_0t sample) and PP/EPR blend film samples filled with 0.001 wt.% Ca-Pim (i.e. PN_1t sample)

and 0.001 wt.% Ca-Sub (i.e. PN$_2$t sample) which were crystallized isothermally at 130°C

(a)

(b)

(c)
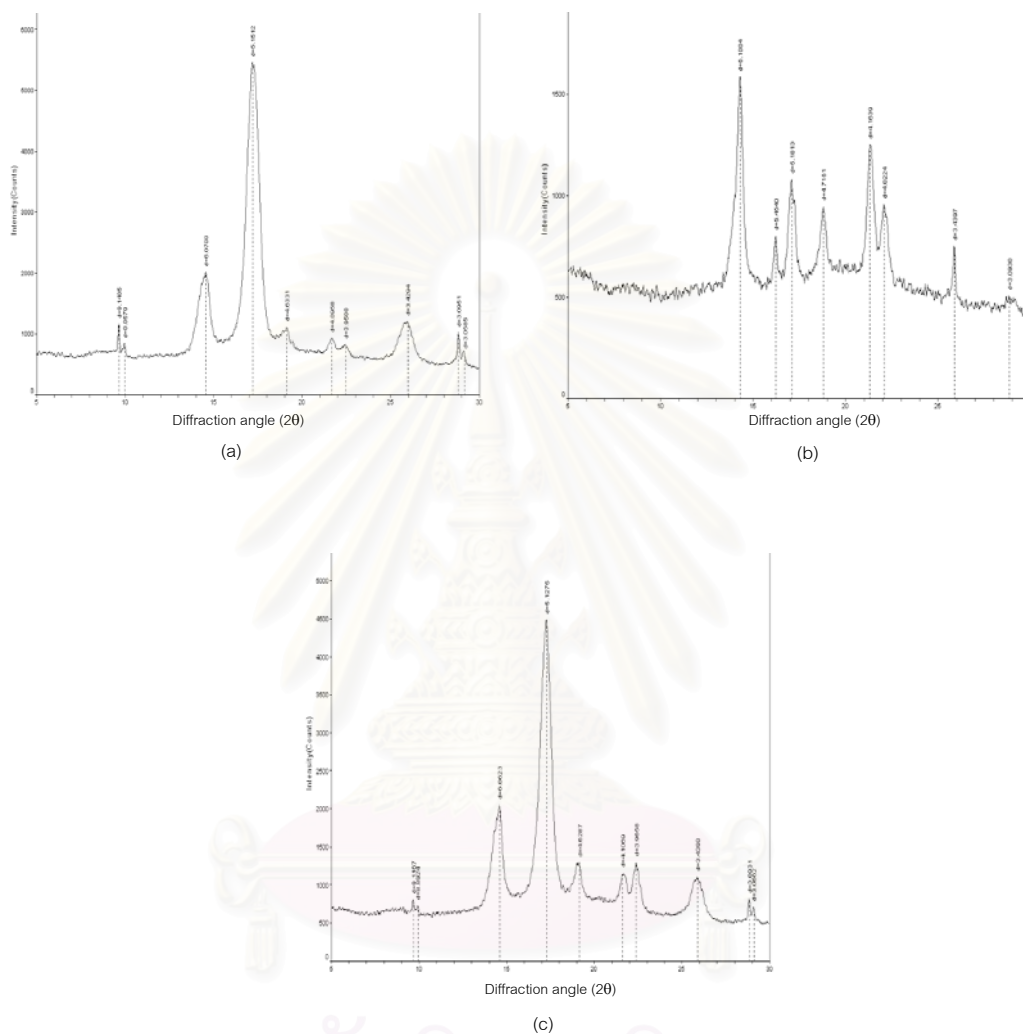
Figure 4.5 (a-c) WAXD diagrams of the unfilled PP/EPR blend, PN$_0$t sample (a), Ca-Pim filled PP/EPR blend PN$_1$t sample, (b) and Ca-Sub filled PP/EPR blend PN$_2$t sample, which crystallization with isothermal temperature at 130 ^{O}C

From Figure 4.5, it can be observed that the PP/EPR blend film sample filled with 0.001 wt.% Ca-Pim exhibited the diffraction peaks associated with the β-phase, with the K-value being calculated to be about 0.10, while the film sample filled with 0.001 wt.% Ca-Sub showed no such peaks.
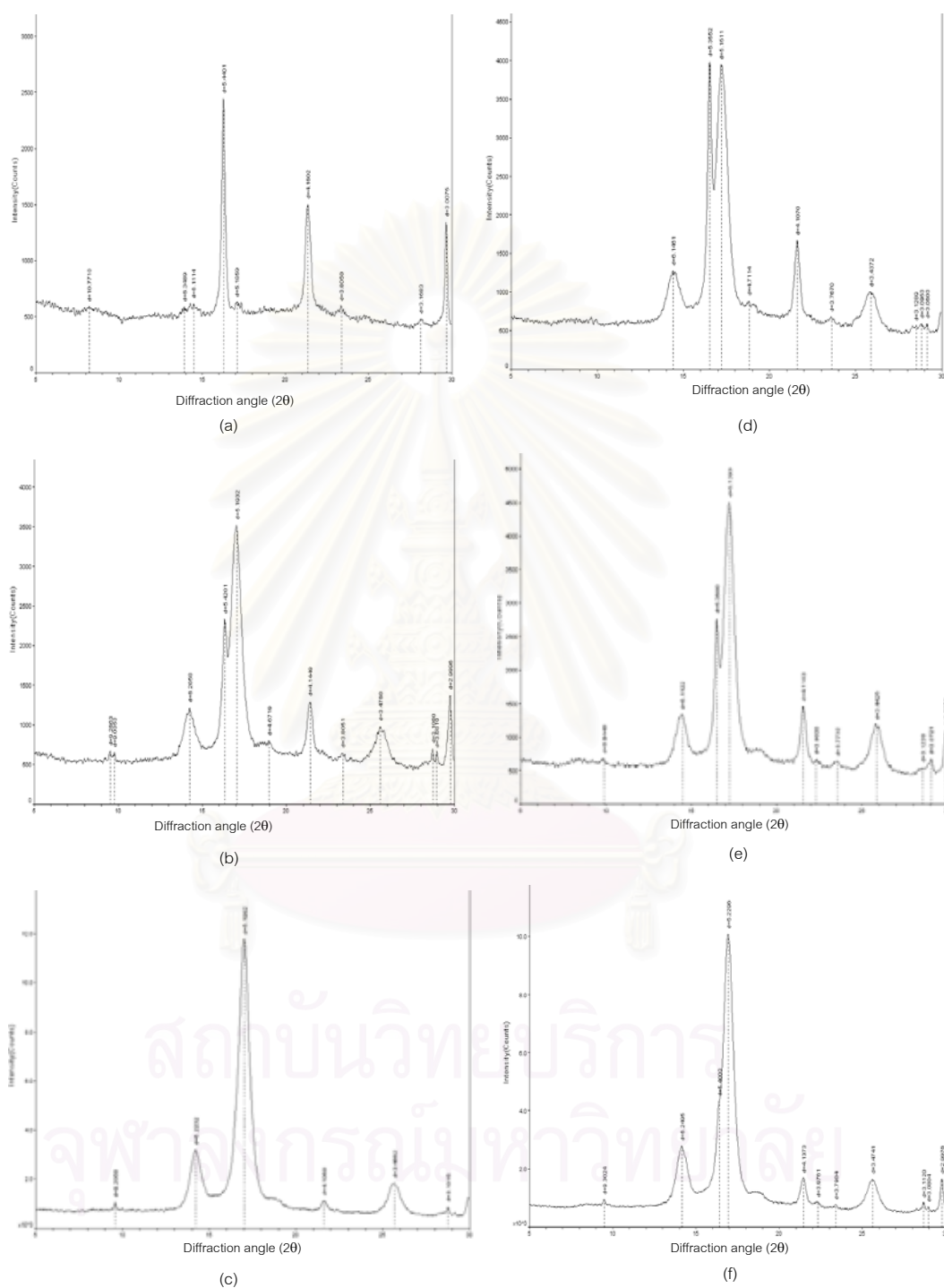
Figure 4.6 WAXD diagrams of μm-CaCO$_3$-filled PP/EPR blend containing 5 (a), 10 (b), 15 wt.% (c) and nm-CaCO$_3$-filled PP/EPR blend containing 5 (d), 10 (e), and 15 wt.% (f), which crystallization with isothermal temperature at 130°C
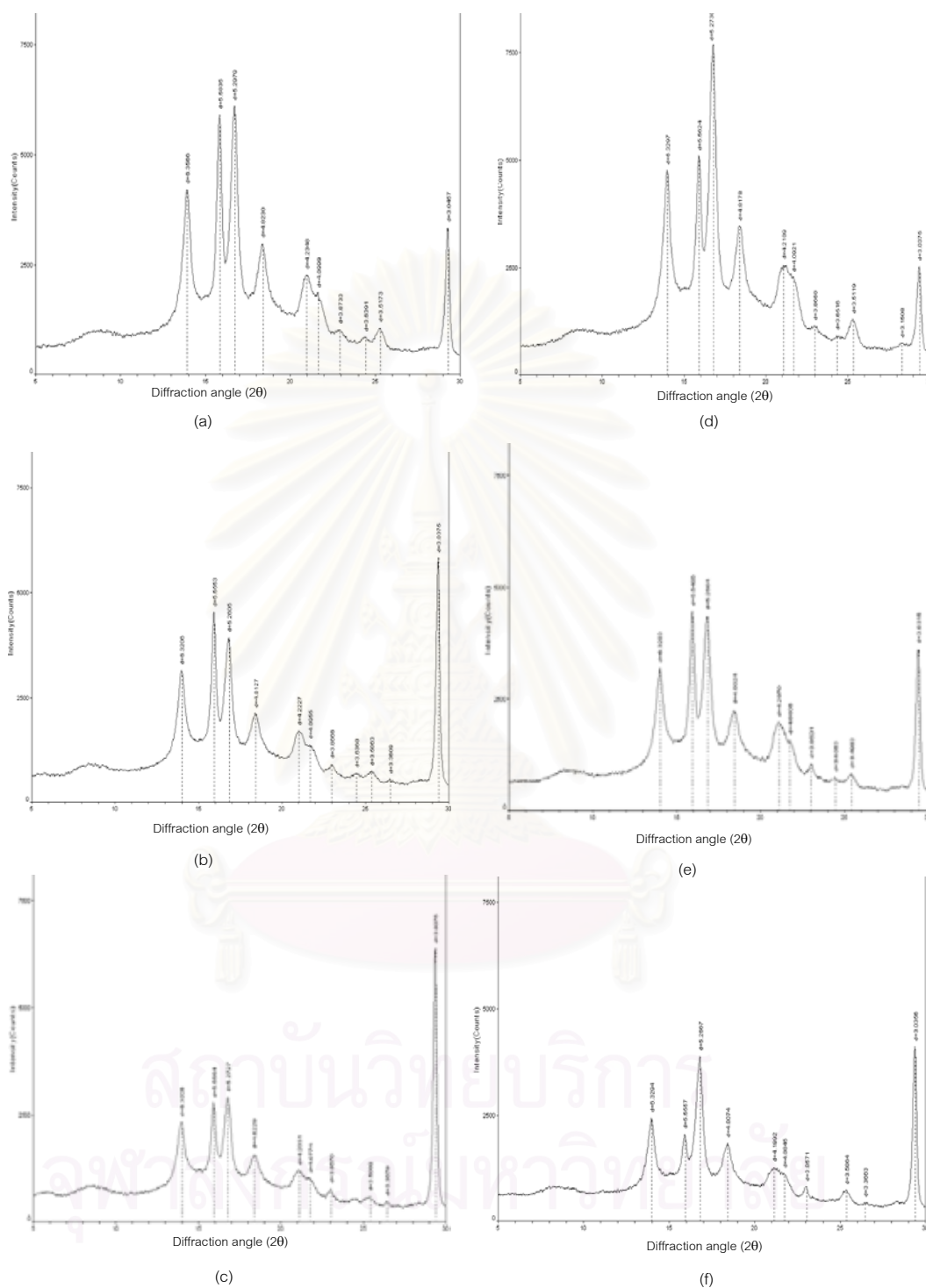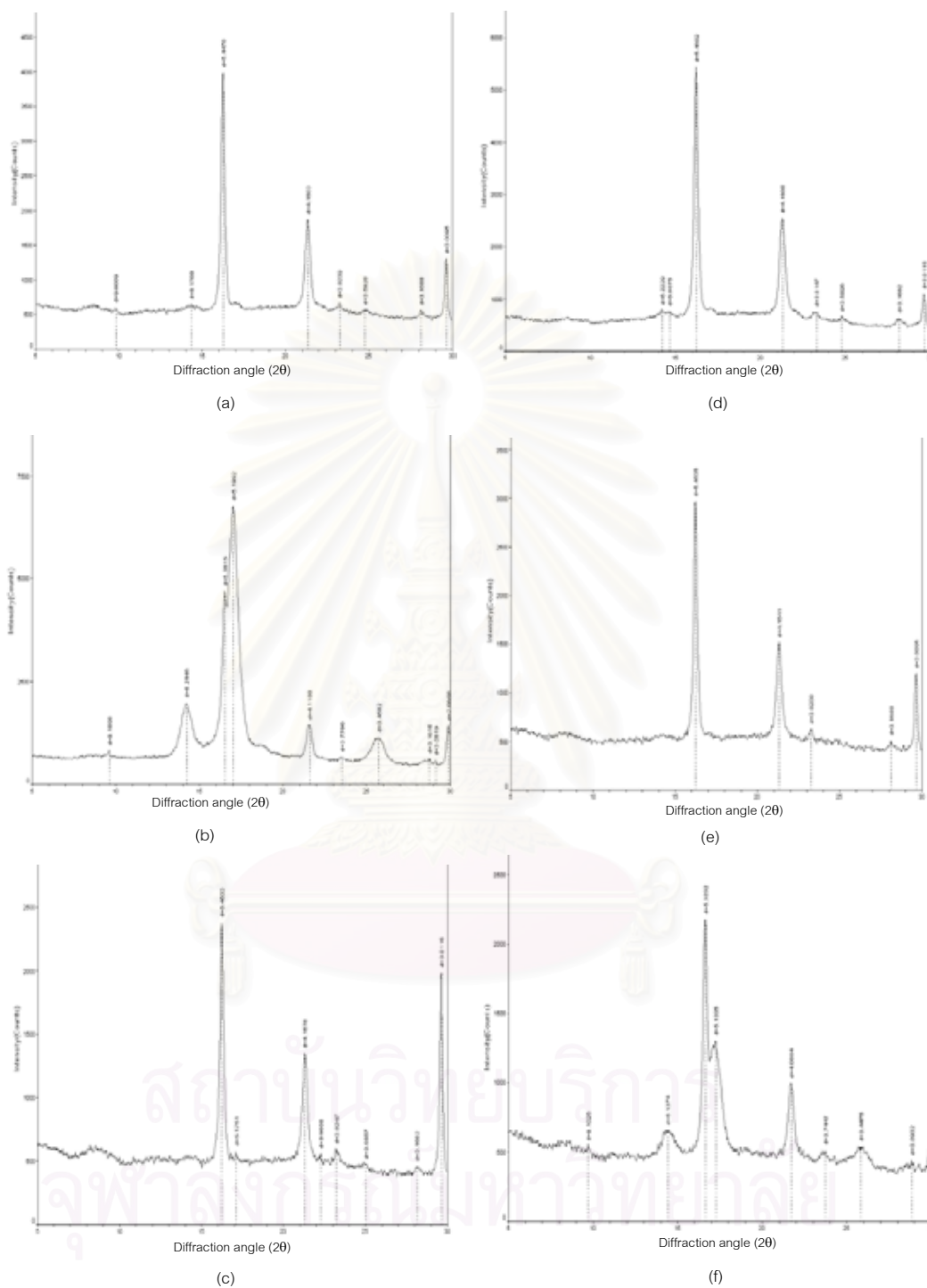
Figure 4.7 The WAXD diagrams of 0.001 wt.% Ca-Pim, and μm- CaCO$_3$ containing 5 (a), 10 (b) and 15 wt.%(c) and 0.001 wt.% Ca-Pim, and nm- CaCO$_3$ containing 5 (d), 10 (e) and 15 wt.% (f) in PP/EPR blend which crystallization with isothermal temperature at 130°C

Figure 4.6 shows WAXD diagrams of the film samples filled with both micro- and nanoparticles of $CaCO_3$ in various contents ranging from 5 to 15 wt.%. Again, these film samples were isothermally crystallized at 130°C.

Figure 4.7 shows WAXD diagrams of the film samples filled with 0.001 wt.% and both micro- and nanoparticles of $CaCO_3$ in various contents ranging from 5 to 15 wt.%. Again, these film samples were isothermally crystallized at 130°C. All of the quantitative analytical results to arrive at the K-values for the WAXD diagrams are shown in Figures 4.6 and 4.7 are summarized in Table 4.7.

Table 4.7 K-value of 0.001 wt.% Ca-Pim, and $CaCO_3$ (μm and nm) containing 5,10, and 15 wt.%-filled PP/EPR blend, which were crystallized with isothermal temperature at 130^OC

Sample code	Ca-Pim (wt.%)	$CaCO_3$(μm) (wt.%)	$CaCO_3$(nm) (wt.%)	H_β	$H_{\alpha 1}$	$H_{\alpha 2}$	$H_{\alpha 3}$	K-value
PN_0C_1t	0	5	0	1901	101	63	0	0.92
PN_0C_2t	0	10	0	1632	558	2623	106	0.33
PN_0C_3t	0	15	0	0	2105	10242	0	0
PN_0Cn_1t	0	0	5	3188	545	2935	87	0.47
PN_0Cn_2t	0	0	10	2004	645	3523	0	0.32
PN_0Cn_3t	0	0	15	3098	1790	8632	0	0.23
PN_1C_1t	0.001	5	0	3397	91	1259	0	0.72
PN_1C_2t	0.001	10	0	3735	1151	5637	0	0.35
PN_1C_3t	0.001	15	0	1874	0	57	0	0.97
PN_1Cn_1t	0.001	0	5	4728	99	0	0	0.98
PN_1Cn_2t	0.001	0	10	2427	0	0	0	1.00
PN_1Cn_3t	0.001	0	15	1507	166	734	0	0.63

Note : $H_{\alpha 1}$, $H_{\alpha 2}$, $H_{\alpha 3}$ are intensities of α-diffraction peaks corresponding to angle θ = 7.1^O, 8.5^O, and 9.4^O, and $H_{\beta 1}$ is the intensity of β-diffraction peaks corresponding to angle θ = 8.1^O

According to Figures 4.6, 4.7 and Table 4.6, it is clearly seen that, without the addition of Ca-Pim, the K-value of the film samples filled with both types of $CaCO_3$ particles was found to decrease with increasing the filler content. It has been reported by McGenity et al. [24] that the presence of $CaCO_3$ particles favors the formation of β-phase in PP homopolymer. The addition of 40% stearate-coated $CaCO_3$ to the PP matrix yields a K-value of about 0.12 whereas for the unfilled PP polymer the β-phase was 0.055.

For the film samples filled with 0.001 wt.% and $CaCO_3$ micro- and nanoparticles, the amount of the β-crystalline formed was high, especially for the one that was filled with 10 wt.% nm-$CaCO_3$ (i.e. PN_1Cn_2t sample) which exhibited the K-value of about 1.0. The results indicated that the presence of both Ca-Pim and $CaCO_3$ particles (especially the nanosized ones) helped promote the formation of the β-phase within the PP/EPR blend matrix. Table 4.8 summarizes the melting characteristics of the neat PP/EPR blend film sample, and the film samples that either contained only 0.001 wt.% Ca-Pim or Ca-Sub or 0.001 wt.% Ca-Pim and $CaCO_3$ micro- and nanoparticles of varying content (i.e. 5, 10, or 15 wt.%). Again, these film samples were isothermally crystallized at a temperature of 130°C.

Table 4.8 The melting characteristics of unfilled PP/EPR blend, Ca-Pim filled PP/EPR blend, Ca-Sub filled PP/EPR blend and Ca-Pim and $CaCO_3$ (μm and nm) filled PP/EPR blend crystallized at 130^OC

Sample	Nucleating agent (wt.%)		Filler (wt.%)		T_m (β) (^{O}C)	T_m (α) (^{O}C)
	Ca-Pim	Ca-Sub	$CaCO_3$(μm)	$CaCO_3$ (n)		
PN_0t	-	-	-	-	-	166.4
PN_1t	0.001	-	-	-	153.2	165.8
PN_2t	-	0.001	-	-	-	166.2
PN_1C_1t	0.001	-	5	-	153.3	165.6
PN_1C_2t	0.001	-	10	-	153.5	165.0
PN_1C_3t	0.001	-	15	-	153.3	165.6
PN_1Cn_1t	0.001	-	-	5	153.6	165.6
PN_1Cn_2t	0.001	-	-	10	152.8	165.0
PN_1Cn_3t	0.001	-	-	15	153.2	166.0

Note : $H_{\alpha1}$, $H_{\alpha2}$, $H_{\alpha3}$ are intensities of α-diffraction peaks corresponding to angle $\theta = 7.1^O$, 8.5^O, and 9.4^O, and $H_{\beta1}$ is the intensity of β-diffraction peaks corresponding to angle $\theta = 8.1$

According to Table 4.8, it is obvious that only one endothermic peak at about 166°C was observed for neat film sample and the film sample that contained 0.001 wt.% Ca-Sub (i.e. PN_2t sample), which confirmed no presence of the β-phase. On the contrary, all other film samples exhibited the endothermic peaks at about 153 and 165-166°C associated with the melting of the β- and the α-phase, respectively.

4.5 The influence of thermal conditions on spherulitic structure

In this study, an optical microscope was used to investigate the spherulitic morphology of the isothermally-crystallized film samples. Figure 4.8 shows optical micrographs of neat PP/EPR blend film sample and the film samples containing either 0.001 wt.% Ca-Pim or 0.001 wt.% Ca-Sub that were isothermally crystallized

at 130°C. According to Figure 4.8, both the neat PP/EPR film sample and the film sample containing 0.001 wt.% Ca-Sub (see Figure 4.8 a and c) displayed dark Maltese cross belonging to the α-phase, while the rather bright hedrites of the β-phase can be observed in the film sample containing 0.001 wt.% Ca-Pim (see Figure 4.8b).

Figure 4.9 shows optical micrographs of the PP/EPR blend film samples containing 0.001 wt.% Ca-Pim which were isothermally crystallized at 130 and 150°C, respectively. From Figure 4.9, β-spherulitic structure was observed at the crystallization of 130°C as bright hedrites, but, when the sample was crystallized at 150°C, the bright hedrites associated to the β-crystals disappeared. Theoretically, the upper temperature limit for the observation of the β-phase in PP was reported to be about 140°C. Above this temperature the α nuclei were formed by secondary $\beta\alpha$ nucleation on the surface of the growing β-spherulites. These α nuclei can grow into α-spherulites segments, which can reach smaller or larger size, depending on the growing time. If the crystallization time is long, these α segments can encompass the original β-spherulites which result is a mixed polymorphic composition. Varga et al. [27] reported that the samples filled Ca-Pim crystallized into nearly pure β-PP up to 135°C, above which a significant α-PP content was obtained.

(a)

Maltese cross

(b)

Bright hedrites

(c)
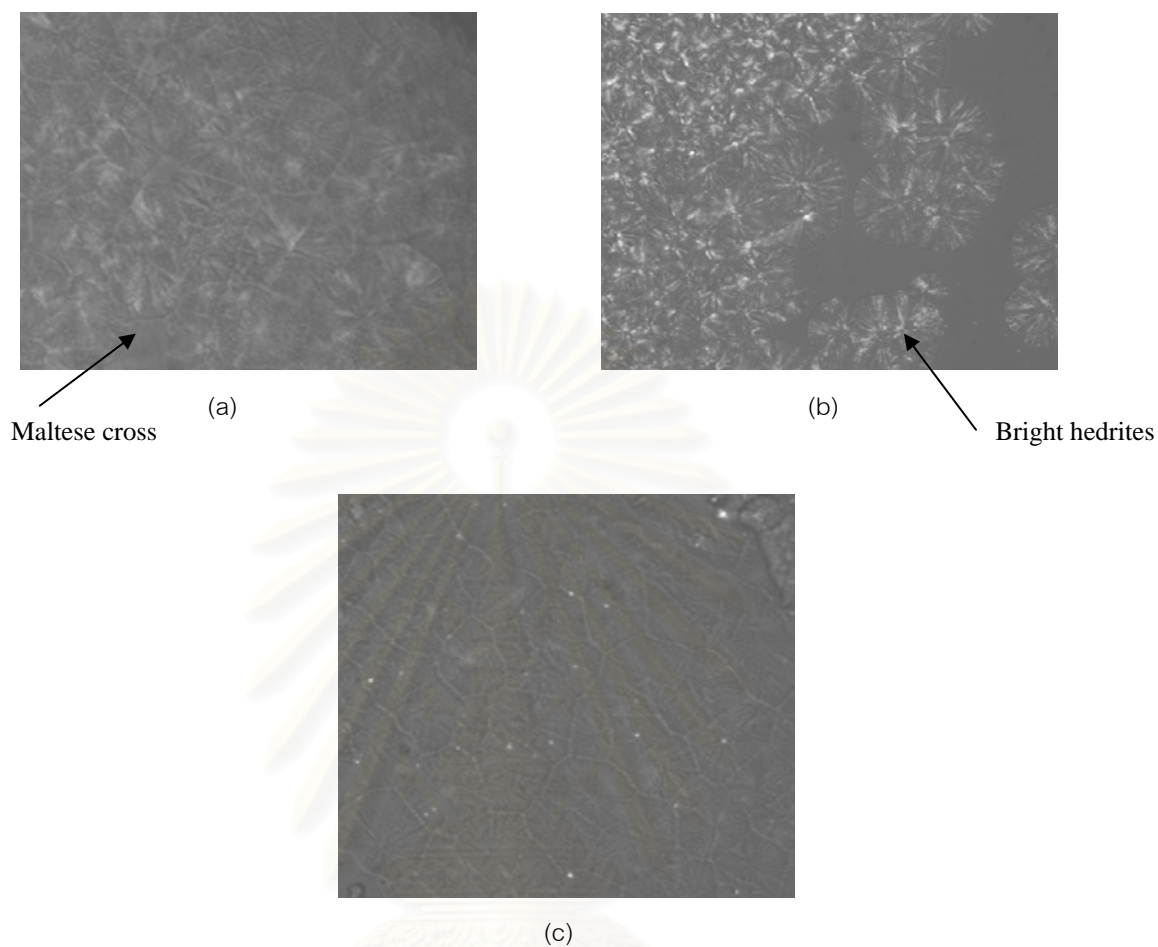
Figure 4.8 Optical micrographs of unfilled PP/EPR blend (a), 0.001 wt.% Ca-Pim filled PP/EPR blend (b) and 0.001 wt.% Ca-Sub filled PP/EPR blend (c) crystallized at 130^OC.

(a)

(b)
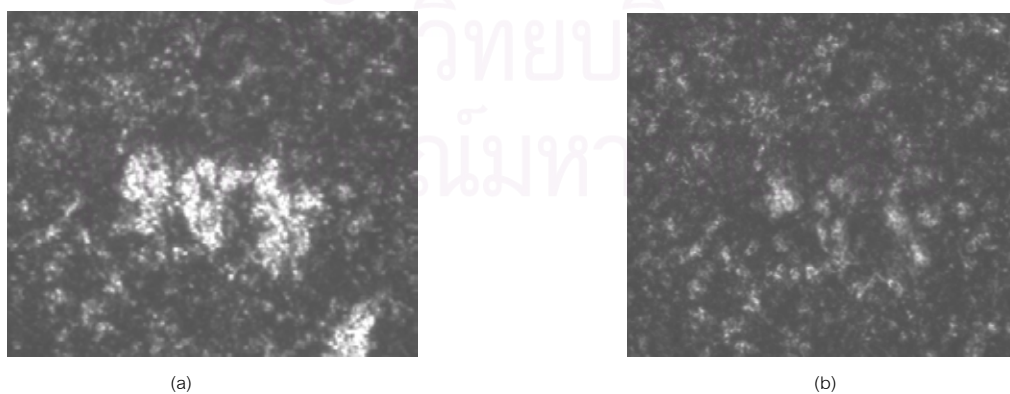
Figure 4.9 Optical micrographs of 0.001 wt.% Ca-Pim filled PP/EPR blend crystallized at 130^OC (a) and 150^OC(b).

CHAPTER V

CONCLUSIONS AND FUTURE DIRECTION

5.1 Conclusions

Based on the experimental results, bicomponent of calcium stearate and pimelic acid (Ca-Pim), promoted β-crystalline in PP/EPR blend as indicated by wide-angle X-ray diffraction measurement. It was found that calcium carbonate ($CaCO_3$) promoted β-crystalline and improved both tensile modulus and flexural modulus. Further investigation revealed that 0.001 wt.% Ca-Pim and 5 wt.% nano-$CaCO_3$ had the highest notched Izod impact strength and improved both tensile and flexural modulus. The k-value of about 0.3 and higher than that of $CaCO_3$ without Ca-Pim was obtained. The β-crystalline formation was confirmed by differential scanning calorimetry (DSC) which presented as an endothermic melting peak at 153 ^{O}C and 169 ^{O}C.

The effects of isothermal crystallization of Ca-Pim and $CaCO_3$ at 130 ^{O}C was investigated. The results showed that the 0.001 wt.% Ca-Pim and $CaCO_3$ (0.8 μm and 40 nm) promoted β-crystalline. The highest k-value at of 1 (completed β-crystalline form) for the composites containing 0.001 wt.% Ca-Pim and 10 wt.% nano- $CaCO_3$ was achieved.

5.2 Future direction

1) To find out appropriate fillers acted as nucleating agents (e.g. mica, glass reinforce, silica) which provides the highest k-value and tensile strength.

2) Based on the research results, it is interesting to apply this formulation to produce actual products that need high tensile modulus, flexural modulus and impact strength. Applications in automobile, electronic and consumer product fields are worth investigated.

REFERENCES

1. Michael, J. B. <u>Handbook of Polypropylene and Polypropylene composites</u>. Amsterdam: Elsevier, **1999**, pp.2-14.

2. Nicholas, P. C. <u>Handbook of Polymer Science and Technology.</u> London: Chapman & Hall.**, 1989**, pp.507-512.

3. Padden, F. J., and Keith, H. D. Spherulitic Crystallization in Polypropylene. <u>J. Appl. Polym. Sci.</u> 30 (1959): 1479-1484.

4. Addink, E. J. and Beintema, J. Polymorphism of Crystalline Polypropylene. <u>Polymer</u> 2 (1961): 185-193.

5. Cho, K., Saheb, D. N., Choi, J. and Yang H. Real Time Situ X-ray Diffraction Studies on the Melting Memory Effect in the Crystallization of β-Isotactic Polypropylene. <u>Polymer</u> 43 (2001): 1407-1416.

6. Turner-Jones, A., Aizlewood, J. M., and Beckeett, D. R. Crystallization Forms of Isotactic Polyprolylene. <u>Makromol. Chem.</u> 75 (1964): 134-154.

7. Varga, J. <u>Polypropylene Structure Blend and Composite.</u> London: Chapman & Hall., **1995**, pp. 68-71.

8. Asano, T., and Fugiwara Y. Plastic Deformation of Oriented Lamellae: 1. Cold Rooling of β-Phase Isotactic Polypropylene. <u>Polymer</u> 19 (1977): 99-108.

9. Yoshida, T., Asano, T., and Fugiwara, Y. Plastic Deformation of Oriented Lamellae: 3. Drawing Behaviour of β-Phase Isotactic Polypropylene. <u>Polymer</u> 42 (1983): 925-929

10. Fugiwara, Y., Goto, T., and Yamashita Y. Comparison of Premelting and Recrystallization Behaviour of β-Phase Isotactic Polypropylene by Heating and Cooling at Difference Rates. Polymer 28 (1987): 1253-1256

11. Garbarczyk, J., and Paukszta, D. Influence of Additives on the Structure and Properties of Polymer: 2. Polymorphic Transitions of Isotactic Polypropylene caused by Aminosulphur Compounds. Polymer 22 (1981): 562-564.

12. Binsbergen, F. L., and De Lange, B. G. M. Morphology of Polypropylene Crystallized from the Melt. Polymer 9 (1968) : 23-40.

13. Jingjiang, L., Xiufen, W., and Qipeng, G. The β-Crystalline form of Wollastonite Filled Polypropylene. Polymer 41 (1990): 2829-2835.

14. Varga, J. β-Modification of Isotactic Polypropylene: Preparation, Strucrure, Processing, Properties, and Application. J. Macromol. Sci. Phys. 41 (2002): 1121-1171.

15. Devaux, E., and Chabert, B. Nature and Origin of the Transcrystalline Interphase of Polypropylene/Glass Fibre Composites after a Shear Stress. Polym. Comm. 32 (1991): 464-468.

16. Varga, J., and Karger-Kocsis, J. Direct Evidence of Row-Nucleated Cylindritic Crystallization in Glass Fiber-Reinforced Polypropylene Composites. Polym. Bull. 30 (1993): 105-110.

17. Norton, D. R, and Keller, A. The Sherulitic and Lamellar Morphology of Melt-Crystallized Isotactic Polypropylene. Polymer 26 (1985): 704-715.

18. Varga, J., Supermolecule Structure of Isotactic Polypropylene. J. Mater. Sci. 27 (1992): 2557-2579.

19. Shi, G., Zhang, X., Qiu, Z. Crystallinzation Kinetics of β-Phase Polypropylene. <u>Mackromol. Chem.</u> 193 (1992): 583-591.

20. Phillips, R. A. and Wolkowicz, M.D. <u>Polypropylene Handbook</u> London: Chapman & Hall., **1996**, pp.134-178.

21. Mei, R., H., Xin, G. L., and Bo-Rong, F. β-Nucleator and β-crystalline Form of Isotactic Polypropylene. <u>J. Appl. Polym. Sci</u>. 56 (1995): 1323-1337.

22. Petermann, J. <u>Polypropylene Structure, Blends and Composites, Structure and Morphology.</u> London: Chapman & Hall., **1994**, pp. 45-93.

23. Geoffrey, P. <u>Polymer Science and Technology.</u> London: Chapman & Hall., **1998**, pp.157-184.

24. McGenity, P. M., Hooper, J. J., Paynter, C. D., Riley, A. M., Nutbeem, C., Elton, N. J. and Adams, J. M. Nucleation and Crystallization of Polypropylene by Mineral Fillers: Relationship to Impact Strength. <u>Polymer</u> 33 (1992): 5215-5224.

25. Sekutowski, D. <u>Polymer Additive.</u> London: Chapman & Hall., **1990**, pp.503-520.

26. Tjong, S. C., Li, R. K., and Chenung, T. Mechanical Behavior of $CaCO_3$ Particulate-Filled β-Crystalline Phase Polypropylene Composites. <u>Polym. Eng. Sci.</u> 37 (1997): 188-172.

27. Varga, J., Mudra, I., and Ehrenatein, G. W. Highly Active Thermally Stable β-Nucleating Agents for Isotactic Polypropylene. <u>J. Appl. Polym. Sci.</u> 74 (1999): 2357-2368.

28. Li, X., Hu, K. C., Ji, M., Huang, Y., and Zhou, G. Calcium Dicarboxylates Nucleation of β-Polypropylene. <u>J. Appl. Polym. Sci.</u> 86 (2002) : 633-638.

29. Sterzynski, T., Calo, P., Lambla, M., and Thomas, M. Trans- and Dimethyl Quinacridone Nucleation of Isotactic Polypropylene. Polym. Eng. Sci. 37 (1997): 1917-1927.

30. Feng, J., Chen, M., Huang, Z., Guo, Y., and Hu, H. Effect of Mineral Additives on the β-Crystalline Form of Isotactic Polypropylene. J. Appl. Polym. Sci. 85 (2002): 1742-1748.

31. Chan, C., Wu, J., Li, J., and Cheung, Y. Polypropylene/Calcium Carbonate Nanocomposites. Polymers 43 (2002): 2981-2992.

32. Todjeman, Ph., Robert, C., Marin, G. and Gerard, P. The Effect of α,β-Crystalline Structure on the Mechanical Properties of Polypropylene. Eur. Phys. J. 4 (2001): 459-465.

33. Li, Y., Fang, Q. F., and Zheng, K. A Study of Internal Friction in Polypropylene (PP) Filled with Nanometer-Scale $CaCO_3$ Particles. J. Mater. Sci. Eng. (2002): 268-272.

34. Kessaraporn, T. Pitt, S. and Supawan, T. Effect of Calcium Stearate and Pimelic acid addition on Mechanical Properties of Heterophasic Isotactic Polypropylene/Ethylene-Propylene Rubber Blends. Polym. Test. 23 (2004): 533-539.

35. Li, J. X., Silverstein, M., Hiltner, A., and Baer, E. The Ductile-to-Quasi-Brittle Transition of Particulate-filled Thermoplastic Polyester. J. Appl. Polym. Sci. 52 (1994): 255-263.

36. Juahsz, P., Varga, J., Belina, K. and Belina, G. Efficiency of β-Nucleating Agents in Polypropylene/α-Olefin Copolymers. J. Macromol. Sci. Phys. 41 (2002): 1173-1189.

APPENDICES

APPENDIX A

A. Mechanical properties of PP/EPR blends filled with different nucleant types at 0.01 wt.%

A.1 Tensile strength of PP/EPR blends filled with different nucleant types at 0.01 wt.%

Table A.1 Tensile strength of PP/EPR blends filled with different nucleant types at 0.01 wt.%

PP/EPR blends filled with	Tensile Strength(MPa)						Data	x	SD
	1st	2nd	3rd	4th	5th	6th			
None(PN_0)	22.26	22.32	21.88	21.9	22.12	22.24	6	22.12	0.190
0.01 wt.% Ca-Pim (PN_1)	21.66	21.54	21.11	21.33	21.11	21.28	6	21.34	0.224
0.01 wt.% Ca-Sub (PN_2)	23.73	23.11	23.78	23.09	23.54	23.43	6	23.45	0.297

A.2 Percentage elongation at yield of PP/EPR blends filled with different nucleant types at 0.01 wt.%

Table A.2 Percentage elongation at yield of PP/EPR blends filled with different nucleant types at 0.01 wt.%

PP/EPR blends filled with	Elongation at yield (%)						Data	x	SD
	1st	2nd	3rd	4th	5th	6th			
None(PN_0)	6.6	6.55	6.78	6.72	6.7	6.58	6	6.66	0.091
0.01 wt.% Ca-Pim (PN_1)	7.9	7.65	7.68	7.72	7.84	7.75	6	7.76	0.096
0.01 wt.% Ca-Sub (PN_2)	6.45	6.52	6.64	6.68	6.54	6.57	6	6.57	0.083

A.3 Flexural Modulus of PP/EPR blends filled with different nucleant types at 0.01 wt.%

Table A.3 Flexural Modulus of PP/EPR blends filled with different nucleant types at 0.01 wt.%

PP/EPR blends filled with	Flexural Modulus (MPa)						Data	x	SD
	1st	2nd	3rd	4th	5th	6th			
None(PN_0)	996	1017	1003	991	999	1008	6	1002.3	9.24
0.01 wt.% Ca-Pim (PN_1)	926	901	914	912	921	918	6	915.3	8.62
0.01 wt.%. Ca-Sub (PN_2)	1025	1010	1014	1015	1004	1002	6	1011.7	8.36

A.4 Izod impact strength of PP/EPR blends filled with different nucleant types at 0.01 wt.%

Table A.4 Izod impact strength of PP/EPR blends filled with different nucleant types at 0.01 wt.%

PP/EPR blends filled with	Izod Impact Strength (J/m)						Data	x	SD
	1st	2nd	3rd	4th	5th	6th			
None(PN_0)	39.25	40.61	38.66	41.86	43.12	42.63	6	41.02	1.82
0.01 wt.% Ca-Pim (PN_1)	151.89	150.41	140.63	141.59	140.81	140.42	6	145.07	5.35
0.01 wt.% Ca-Sub (PN_2)	115.86	123.27	121.00	132.07	125.16	125.16	6	123.47	5.93

APPENDIX B

B. Mechanical properties of kaolin-filled and different nucleant types PP/EPR blend.

B.1 Tensile strength of kaolin-filled and different nucleant types PP/EPR blend.

Table B.1 Tensile strength of kaolin-filled and different nucleant types PP/EPR blend

Sample code	Nucleator content (wt.%)			Tensile Strength (MPa)						Data	x	SD
	kaolin	Ca-Pim	Ca-Sub	1st	2nd	3rd	4th	5th	6th			
PN_0K_1	5	0	0	22.77	22.79	22.75	22.81	22.74	22.80	6	22.77	0.03
PN_0K_2	10	0	0	22.02	22.46	22.54	22.41	22.36	22.04	6	22.31	0.22
PN_0K_3	15	0	0	19.58	19.40	19.49	19.28	19.32	19.43	6	19.42	0.11

B.2 Percentage elongation at yield of kaolin-filled and different nucleant types PP/EPR blend.

Table B.2 Percentage elongation at yield of kaolin-filled and different nucleant types PP/EPR blend.

Sample code	Nucleator content (wt.%)			Elongation at yield (%)						Data	x	SD
	kaolin	Ca-Pim	Ca-Sub	1st	2nd	3rd	4th	5th	6th			
PN_0K_1	5	0	0	6.1	6.34	6.15	6.28	6.16	6.12	6	6.19	0.10
PN_0K_2	10	0	0	5.47	5.55	5.56	5.44	5.6	5.55	6	5.53	0.06
PN_0K_3	15	0	0	5.44	5.42	5.52	5.58	5.51	5.58	6	5.51	0.07

B.3 Flexural Modulus of kaolin-filled and different nucleant types PP/EPR blend.

Table B.3 Flexural Modulus of kaolin-filled and different nucleant types PP/EPR blend.

Sample code	Nucleator content (wt.%)			Flexural Modulus (MPa)						Data	x	SD
	kaolin	Ca-Pim	Ca-Sub	1st	2nd	3rd	4th	5th	6th			
PN_0K_1	5	0	0	1019	1030	1037	1027	1025	1032	6	1054.5	6.19
PN_0K_2	10	0	0	1181	1184	1169	1177	1188	1178	6	1179.5	6.53
PN_0K_3	15	0	0	1256	1261	1269	1268	1251	1246	6	1258.5	9.22

B.4 Izod impact strength of of kaolin-filled and different nucleant types PP/EPR blend.

Table B.4 Izod impact strength of of kaolin-filled and different nucleant types PP/EPR blend**.**

Sample code	Nucleator content (wt.%)			Izod Impact Strength (J/m)						Data	x	SD
	kaolin	Ca-Pim	Ca-Sub	1st	2nd	3rd	4th	5th	6th			
PN_0K_1	5	0	0	128.68	120.64	118.36	124.80	119.77	123.19	6	122.57	3.46
PN_0K_2	10	0	0	78.12	83.74	83.61	87.45	85.21	84.08	6	83.70	2.28
PN_0K_3	15	0	0	150.57	149.28	146.61	149.94	150.52	148.76	6	149.28	1.48

APPENDIX C

C. Mechanical properties of calcium carbonate-filled and different nucleant types PP/EPR blend.

C.1 Tensile strength of calcium carbonate -filled and different nucleant types PP/EPR blend.

Table C.1 Tensile strength of calcium carbonate -filled and different nucleant types PP/EPR blend

Sample code	Nucleator content (wt.%)			Tensile Strength (MPa)						Data	x	SD
	$CaCO_3$	Ca-Pim	Ca-Sub	1st	2nd	3rd	4th	5th	6th			
PN_0C_1	5	0	0	20.77	19.26	20.67	20.57	20.27	20.3	6	20.31	0.55
PN_0C_2	10	0	0	20.85	20.51	20.52	20.25	20.18	20.65	6	20.49	0.25
PN_0C_3	15	0	0	19.53	19.09	19.03	18.96	19.1	19.19	6	19.15	0.20
PN_1C_1	5	0.01	0	20.49	19.66	19.61	19.96	19.85	19.8	6	19.90	0.32
PN_1C_2	10	0.01	0	19.34	19.43	19.05	18.72	19.22	19.2	6	19.16	0.25
PN_1C_3	15	0.01	0	18.02	17.64	17.6	17.65	17.54	17.48	6	17.66	0.19

C.2 Percentage elongation at yield of calcium carbonate -filled and different nucleant types PP/EPR blend.

Table C.2 Percentage elongation at yield of calcium carbonate -filled and different nucleant types PP/EPR blend.

Sample code	Nucleator content (wt.%)			Elongation at yield (%)						Data	x	SD
	$CaCO_3$	Ca-Pim	Ca-Sub	1st	2nd	3rd	4th	5th	6th			
PN_0C_1	5	0	0	6.82	6.78	7.1	6.89	7	7	6	6.93	0.12
PN_0C_2	10	0	0	6.97	6.85	6.81	6.95	6.92	6.9	6	6.90	0.06
PN_0C_3	15	0	0	5.17	5.26	5.1	5.14	5.22	5.2	6	5.18	0.06
PN_1C_1	5	0.01	0	7.84	7.62	7.89	7.83	7.65	7.76	6	7.77	0.11
PN_1C_2	10	0.01	0	7.76	7.8	7.74	7.81	7.68	7.7	6	7.75	0.05
PN_1C_3	15	0.01	0	5.17	5.2	5.12	5.14	5.23	5.2	6	5.18	0.04

71

C.3 Flexural Modulus of calcium carbonate -filled and different nucleant types PP/EPR blend.

Table C.3 Flexural Modulus of calcium carbonate -filled and different nucleant types PP/EPR blend.

Sample code	Nucleator content (wt.%)			Flexural Modulus (MPa)						Data	x	SD
	$CaCO_3$	Ca-Pim	Ca-Sub	1st	2nd	3rd	4th	5th	6th			
PN_0C_1	5	0	0	1036	1041	1030	1023	1034	1026	6	1031.67	6.65
PN_0C_2	10	0	0	1141	1134	1130	1133	1137	1145	6	1136.67	5.54
PN_0C_3	15	0	0	1254	1241	1252	1246	1247	1252	6	1248.67	4.89
PN_1C_1	5	0.01	0	1001	1016	991	995	1004	1002	6	1001.5	8.60
PN_1C_2	10	0.01	0	1183	1174	1175	1178	1185	1180	6	1179.2	4.36
PN_1C_3	15	0.01	0	1239	1239	1223	1223	1232	1230	6	1231.0	7.18

C.4 Izod impact strength of of calcium carbonate -filled and different nucleant types PP/EPR blend.

Table C.4 Izod impact strength of of calcium carbonate -filled and different nucleant types PP/EPR blend.

Sample code	Nucleator content (wt.%)			Izod Impact Strength (J/m)						Data	x	SD
	$CaCO_3$	Ca-Pim	Ca-Sub	1st	2nd	3rd	4th	5th	6th			
PN_0C_1	5	0	0	141.79	121.93	119.15	118.29	128.48	117.82	6	124.58	9.31
PN_0C_2	10	0	0	62.02	61.75	61.76	60.46	61.70	59.96	6	61.28	0.85
PN_0C_3	15	0	0	55.42	51.63	54.02	52.49	53.06	54.33	6	53.49	1.37
PN_1C_1	5	0.01	0	80.35	79.89	78.60	78.52	80.53	79.60	6	79.58	0.86
PN_1C_2	10	0.01	0	72.21	66.96	61.78	70.88	71.08	68.55	6	68.57	3.84
PN_1C_3	15	0.01	0	59.22	57.95	64.37	62.68	60.25	61.81	6	61.04	2.36

APPENDIX D

D. Mechanical properties of calcium carbonate(nano)-filled and different nucleant types PP/EPR blend.

C.1 Tensile strength of calcium carbonate -filled and different nucleant types PP/EPR blend.

Table D.1 Tensile strength of calcium carbonate(nano) -filled and different nucleant types PP/EPR blend

Sample code	Nucleator content (wt.%)			Tensile Strength (MPa)						Data	x	SD
	CaCO3	Pim-Cat	Ca-Sub	1st	2nd	3rd	4th	5th	6th			
PN_1Cn_1	5	0.01	0	21.06	20.15	20.18	20.38	20.37	20.4	6	20.42	0.33
PN_1Cn_2	10	0.01	0	19.11	19.41	19.33	19.84	18.92	18.98	6	19.27	0.34
PN_1Cn_3	15	0.01	0	18.88	18.02	17.91	18.02	18.18	18.2	6	18.20	0.35

D.2 Percentage elongation at yield of calcium carbonate (nano)-filled and different nucleant types PP/EPR blend.

Table C.2 Percentage elongation at yield of calcium carbonate(nano) -filled and different nucleant types PP/EPR blend.

Sample code	Nucleator content (wt.%)			Elongation at yield (%)						Data	x	SD
	$CaCO_3$	Ca-Pim	Ca-Sub	1st	2nd	3rd	4th	5th	6th			
PN_1Cn_1	5	0.01	0	6.9	6.87	6.95	6.98	6.86	6.94	6	6.92	0.05
PN_1Cn_2	10	0.01	0	7.74	7.8	7.76	7.72	7.83	7.72	6	7.76	0.04
PN_1Cn_3	15	0.01	0	5.2	5.19	5.11	5.14	5.24	5.12	6	5.17	0.05

D.3 Flexural modulus of calcium carbonate(nano) -filled and different nucleant types PP/EPR blend.

Table D.3 Flexural Modulus of calcium carbonate(nano) -filled and different nucleant types PP/EPR blend.

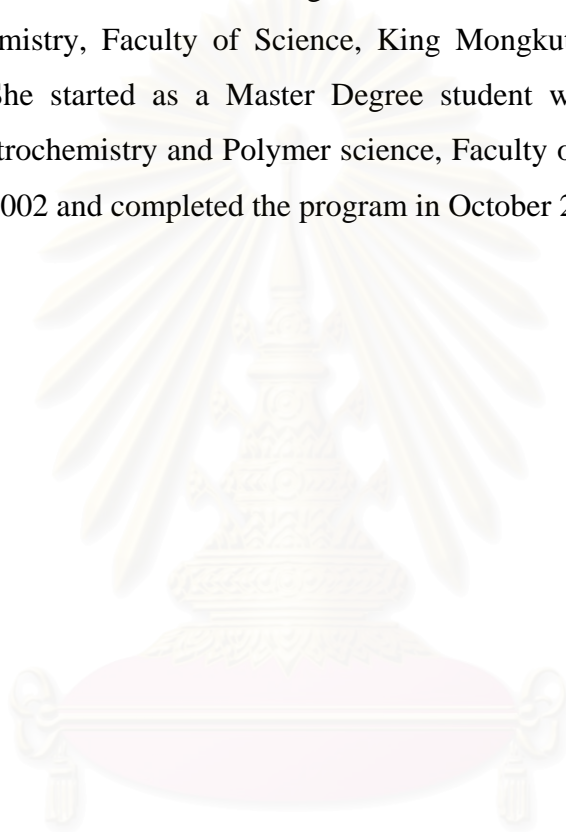| Sample code	Nucleator content (wt.%)			Flexural Modulus (MPa)						Data	x	SD
	$CaCO_3$	Ca-Pim	Ca-Sub	1st	2nd	3rd	4th	5th	6th			
PN_1Cn_1	5	0.01	0	1023	1014	1017	1030	1036	1022	6	1023.7	8.16
PN_1Cn_2	10	0.01	0	1004	1001	1006	1005	1011	1010	6	1006.2	3.76
PN_1Cn_3	15	0.01	0	1110	1097	1093	1107	1120	1106	6	1105.5	9.61

D.4 Izod impact strength of of calcium carbonate(nano) -filled and different nucleant types PP/EPR blend.

Table D.4 Izod impact strength of of calcium carbonate (nano) -filled and different nucleant types PP/EPR blend.

Sample code	Nucleator content (%wt.)			Izod Impact Strength (J/m)						Data	x	SD
	$CaCO_3$	Ca-Pim	Ca-Sub	1st	2nd	3rd	4th	5th	6th			
PN_1Cn_1	5	0.01	0	143.39	143.05	131.57	140.61	136.90	135.78	6	138.55	4.62
PN_1Cn_2	10	0.01	0	131.64	125.16	129.16	125.07	121.19	126.55	6	126.46	3.62
PN_1Cn_3	15	0.01	0	110.65	99.22	99.22	95.35	101.87	102.32	6	101.44	5.15

VITAE

Miss Ratchaneekun Bunnuklap was born in Phattalung, Thailand, on July 19th, 1976. She received Bachelor Degree of Science in 1999 from Department of Industrial Chemistry, Faculty of Science, King Mongkut Institute of Technology Ladkrabang. She started as a Master Degree student with a major in Polymer, Program of Petrochemistry and Polymer science, Faculty of Science, Chulalongkorn University in 2002 and completed the program in October 2005.